

FERMILAB-Conf-02/053-T  
 MCTP-02-16  
 SCIPP-02/03  
 BNL-69066  
 DESY 02-050  
 hep-ph/0203229  
 March 2002

## Executive Summary of the Snowmass 2001 Working Group (P1) “ELECTROWEAK SYMMETRY BREAKING”

Marcela Carena,<sup>1,\*</sup> David W. Gerdes,<sup>2,†</sup> Howard E. Haber,<sup>3,‡</sup> André S. Turcot,<sup>4,§</sup> and Peter M. Zerwas<sup>5,¶</sup>

<sup>1</sup>*Theoretical Physics Department, Fermi National Accelerator Laboratory, Batavia, Illinois 60510-0500, USA*

<sup>2</sup>*Department of Physics, University of Michigan, Ann Arbor, Michigan 48109-1120, USA*

<sup>3</sup>*Santa Cruz Institute for Particle Physics, University of California, Santa Cruz, California 95064, USA*

<sup>4</sup>*Brookhaven National Laboratory, Upton, New York 11973-5000, USA*

<sup>5</sup>*Deutsches Elektronen-Synchrotron, D-22603 Hamburg, Germany*

(Dated: January 30, 2020)

In this summary report of the 2001 Snowmass Electroweak Symmetry Breaking Working Group, the main candidates for theories of electroweak symmetry breaking are surveyed, and the criteria for distinguishing among the different approaches are discussed. The potential for observing electroweak symmetry breaking phenomena at the upgraded Tevatron and the LHC is described. We emphasize the importance of a high-luminosity  $e^+e^-$  linear collider for precision measurements to clarify the underlying electroweak symmetry breaking dynamics. Finally, we note the possible roles of the  $\mu^+\mu^-$  collider and VLHC for further elucidating the physics of electroweak symmetry breaking.

### I. THE ORIGIN OF ELECTROWEAK SYMMETRY BREAKING

#### A. Introduction

Deciphering the mechanism that breaks the electroweak symmetry and generates the masses of the known fundamental particles is one of the central problems of particle physics [1, 2]. This mechanism will be explored by experiments now underway at the upgraded proton-antiproton Tevatron collider and in the near future at the Large Hadron Collider (LHC). Once evidence for electroweak symmetry breaking (EWSB) dynamics is obtained, a more complete understanding of the mechanisms involved will require experimentation at future

---

\*carena@fnal.gov

†gerdes@umich.edu

‡haber@scipp.ucsc.edu

§turcot@fnal.gov

¶zerwas@desy.de

$e^+e^-$  linear colliders now under development. In certain scenarios, a  $\mu^+\mu^-$  collider or the next generation of very large hadron colliders after LHC (VLHC) can play an important role in establishing the nature of the mass generation mechanism for the fundamental particles.

The dynamics of electroweak symmetry breaking requires the existence of at least one new particle beyond the presently observed spectrum of the Standard Model. The energy scale associated with electroweak symmetry breaking dynamics must be of order 1 TeV or below in order to preserve the unitarity of the scattering matrix for electroweak gauge bosons [3], a principle guaranteed by quantum mechanics. The specific details of the mechanism realized in nature to break the electroweak symmetry have far-reaching consequences for possible new physics beyond the Standard Model.

The generation of masses for the  $W^\pm$  and  $Z$  gauge bosons is associated with the dynamics of electroweak symmetry breaking. Goldstone bosons, which are massless scalar degrees of freedom, are generated by the symmetry-breaking mechanism and transformed into the longitudinal spin components of the  $W^\pm$  and  $Z$ . At present, the underlying nature of this dynamics is unknown. Two broad classes of electroweak symmetry breaking mechanisms have been pursued theoretically. In one class of theories, electroweak symmetry breaking dynamics is weakly-coupled, while in the second class of theories the dynamics is strongly-coupled.

In theories of weak electroweak symmetry breaking, the symmetry is broken by the dynamics of a weakly-coupled sector of self-interacting elementary scalar fields. These self-interactions give rise to a non-vanishing scalar field in the vacuum. Interactions of the Standard Model fields with this vacuum field generate the masses of the gauge bosons, quarks and leptons. In addition, the physical particle spectrum also contains massive scalars—the Higgs bosons [1, 4]. All fields remain weakly interacting at energies up to the grand unification scale which is close to the Planck scale. At energies at and beyond the Planck scale, gravitational interactions become as important as the strong and electroweak interactions, and must be incorporated in the theory in a consistent quantum mechanical way. In the weakly-coupled approach to electroweak symmetry breaking, the Standard Model is very likely embedded in a supersymmetric theory [5] in order to stabilize the large gap between the electroweak and the grand unification (and Planck) scales in a natural way [6]. These theories predict a spectrum of Higgs scalars [7], with the lightest Higgs scalar mass below about 135 GeV [8] in the model’s minimal realization.

Alternatively, strong breaking of electroweak symmetry is accomplished by new strong interactions near the TeV scale [2, 9]. In most realizations of this approach, condensates of fermion-antifermion pairs are generated in the vacuum. The interactions of the electroweak gauge bosons with the associated Goldstone modes generate the masses of the gauge bosons. These models typically possess no elementary scalar fields. In some approaches, composite scalar fields, which may resemble physical Higgs bosons, exist in the spectrum and are composed of fermionic constituents. These constituents may be new matter fermions, as in the case of technicolor models [2, 10, 11], or a combination of new heavy quarks and the heavy Standard Model top and bottom quarks, as in the case of top-color models [12, 13]. Quark and lepton masses are generated by introducing either effective Yukawa couplings between the composite scalar fields and the fermion fields or by extending the system by adding new additional gauge interactions that mediate the interactions between the Standard-Model fermions and the new fermions. These theoretical approaches are quite complicated constructs; the simplest realizations are generally in conflict with experimental constraints such as precision electroweak data and flavor changing neutral current bounds.

A new approach to electroweak symmetry breaking has recently been under intense investigation, in which extra space dimensions beyond the usual  $3 + 1$  dimensional spacetime are introduced [14, 15, 16] with char-

acteristic sizes of order  $(\text{TeV})^{-1}$ . In such scenarios, the mechanisms for electroweak symmetry breaking are inherently extra-dimensional, and can result in a phenomenology significantly different from the usual approaches mentioned above. For example, the mass of the Higgs boson may be generated through interactions with Kaluza-Klein states in the bulk of multi-dimensional space-time. In some cases, the Higgs couplings to quarks and leptons may be drastically altered compared with the predictions of the Standard Model [17]. Some models exhibit new scalar fields (*e.g.*, radions) which mix with the Higgs bosons and can result in significant shifts in the Higgs couplings [16, 18, 19]. In all such approaches, new physics must be revealed at the TeV scale or below. Clearly, in order to understand *any* theory of electroweak symmetry breaking dynamics, it is critical to explore and interpret the attendant new TeV-scale physics beyond the Standard Model.

### B. Criteria for Distinguishing among Models of EWSB

Although there is as yet no direct evidence for the nature of electroweak symmetry breaking dynamics, present data can be used to discriminate among the different approaches. For example, precision electroweak data, accumulated in the past decade at LEP, SLC, the Tevatron, and elsewhere, strongly supports the Standard Model with a weakly-coupled Higgs boson [20, 21]. Moreover, the contribution of new physics, which can enter through  $W^\pm$  and  $Z$  boson vacuum polarization corrections, is severely constrained. This fact has already served to rule out several models of strongly-coupled electroweak symmetry breaking dynamics. The Higgs boson contributes to the  $W^\pm$  and  $Z$  boson vacuum polarization through loop effects, and so a Standard Model fit to the electroweak data yields information about the Higgs mass. Present fits indicate that the Higgs mass should be around 100 GeV [with a fractional  $1\sigma$  uncertainty of about 50%], comparable to the direct search upper limit, and must be less than about 200 GeV at 95% CL, as shown in Figure 1a. The electroweak data have improved significantly over the past decade, as shown in Figure 1b, to the extent that the conclusions of the 2001 Snowmass Workshop are considerably sharper than what was possible at the end of the 1996 Snowmass Workshop.

There are some loopholes that can be exploited to circumvent this conclusion. It is possible to construct models of new physics where the goodness of the global Standard Model fit to precision electroweak data is not compromised while the strong upper limit on the Higgs mass is relaxed. In particular, one can construct effective operators [22] or specific models [13, 19, 23] of new physics where the Higgs mass is significantly heavier, but the new physics contribution to the  $W^\pm$  and  $Z$  vacuum polarizations is still consistent with the experimental data. In addition, some have argued that the global Standard Model fit exhibits possible internal inconsistencies [24], which would suggest that systematic uncertainties have been underestimated and/or new physics beyond the Standard Model is required. Thus, although weakly-coupled electroweak symmetry breaking models seem to be favored by the strong upper limit on the Higgs mass, one cannot definitively rule out all other approaches.

Nevertheless, one additional piece of data is very suggestive. Within the supersymmetric extension of the Standard Model, grand unification of the electromagnetic, the weak and the strong gauge interactions can be achieved in a consistent way, strongly supported by the prediction of the electroweak mixing angle at low energy scales with an accuracy at the percent level [25, 26]. The significance of this prediction is not easily matched by other approaches. For example, in strongly-coupled electroweak symmetry breaking models, unification of couplings is not addressed *per se*, whereas in extra-dimensional models it is often achieved by introducing new structures at intermediate energy scales. Unless one is willing to regard the apparent gauge coupling unification as a coincidence, it is tempting to conclude that weak electroweak symmetry breaking is the preferred mechanism,

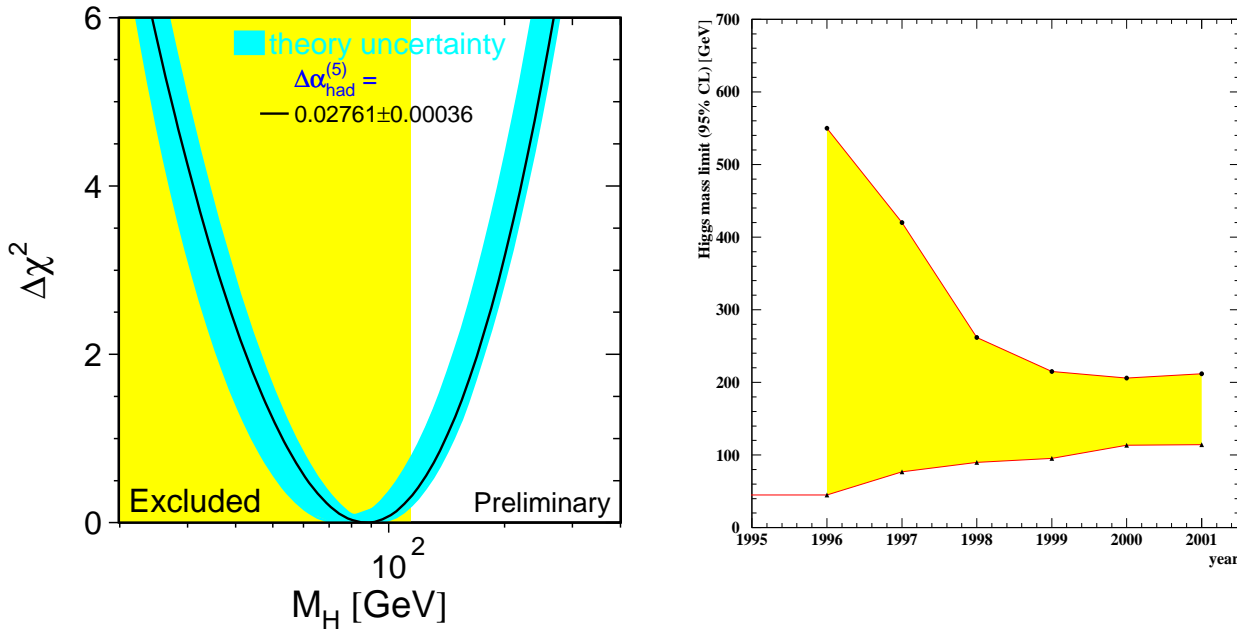


FIG. 1: (a) The “blueband plot” shows  $\Delta\chi^2 \equiv \chi^2 - \chi^2_{\min}$  as a function of the Standard Model Higgs mass [20, 21]. The solid line is a result of a global fit using all data; the band represents the theoretical error due to missing higher order corrections. The rectangular shaded region shows the 95% CL exclusion limit on the Higgs mass from direct searches. (b) The evolution of the bounds on the Standard Model Higgs mass from 1996–2001. The upper boundary corresponds to the 95% CL upper bound on the Higgs mass derived from the global fit to electroweak data, and the lower boundary corresponds to the 95% CL lower bound on the Higgs mass from direct searches.

leading to an expected mass of the lightest Higgs boson below 200 GeV (less than 135 GeV in the simplest supersymmetric models), and a spectrum of additional neutral and charged Higgs bosons with masses up to of order 1 TeV.

## II. EWSB PHYSICS AT PRESENT AND NEAR-FUTURE HADRON COLLIDERS: TEVATRON AND LHC

### A. Standard Model Higgs Boson

After a decade long search for the Standard Model (SM) Higgs boson ( $h_{\text{SM}}$ ) at LEP, Higgs masses up to 114 GeV have been excluded [27]. The next step in the search for Higgs bosons will take place at the Tevatron [28]. In the Higgs mass range below 135 GeV, the most promising signals can be extracted from  $Wh_{\text{SM}}$  and  $Zh_{\text{SM}}$  Higgs-strahlung, in which the gauge bosons decay leptonically and the Higgs boson decays into the  $b\bar{b}$  final state. For Higgs masses above 135 GeV,  $h_{\text{SM}} \rightarrow WW^{(*)}$  becomes the dominant decay mode (the asterisk indicates a virtual  $W$ ). The anticipated Tevatron Higgs discovery reach is illustrated in Figure 2a, and is based on the combined statistical power of the CDF and DØ experiments [28]. The curves shown are obtained by combining the  $\ell\nu b\bar{b}$ ,  $\nu\bar{\nu} b\bar{b}$  and  $\ell^+\ell^- b\bar{b}$  channels using a neural network selection [29] in the low-mass Higgs region ( $90 \text{ GeV} \lesssim m_{h_{\text{SM}}} \lesssim 130 \text{ GeV}$ ), and the  $\ell^\pm\ell^\pm jjX$  and  $\ell^+\ell^-\nu\bar{\nu}$  channels [30] in the high-mass Higgs region ( $130 \text{ GeV} \lesssim m_{h_{\text{SM}}} \lesssim 190 \text{ GeV}$ ). The lower edge of the bands is the calculated threshold; the bands extend upward from these nominal thresholds by 30% as an indication of the uncertainties in  $b$ -tagging efficiency, background

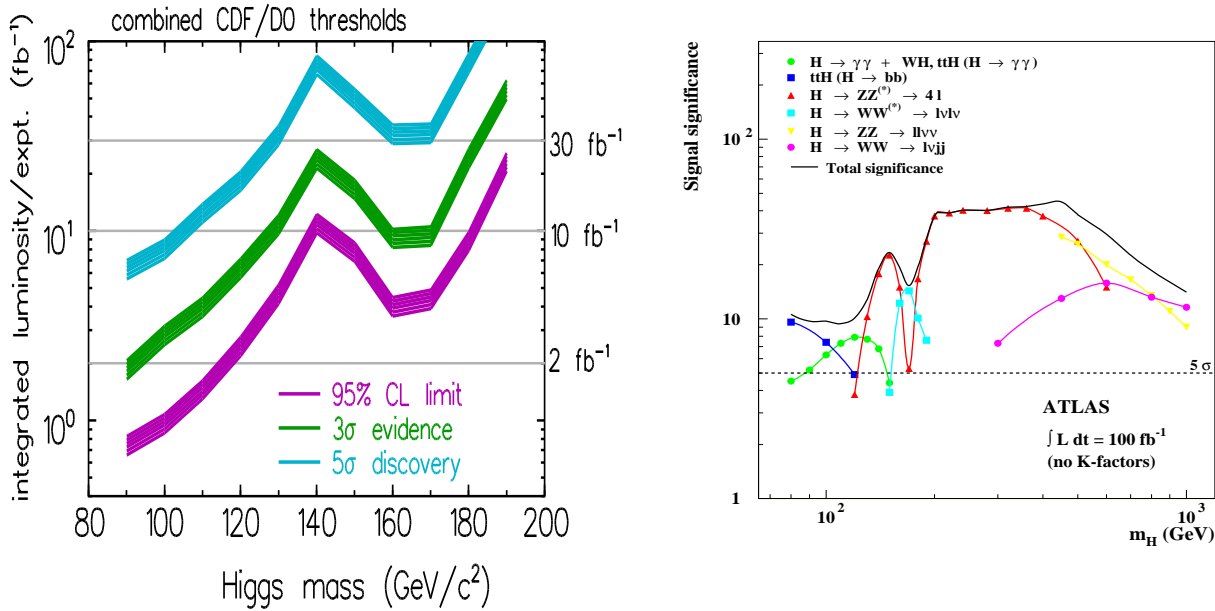


FIG. 2: (a) The integrated luminosity required per Tevatron experiment, to either exclude a Standard Model Higgs boson at 95% CL or observe it at the  $3\sigma$  or  $5\sigma$  level, as a function of the Higgs mass [28]. (b) Higgs significance levels as a function of the Higgs mass for the ATLAS experiment at the LHC, assuming an integrated luminosity of  $100 \text{ fb}^{-1}$  [31].

rate, mass resolution, and other effects. Combining all the indicated channels, the integrated luminosities necessary to rule out the Higgs boson of the Standard Model for a mass below 200 GeV at the 95% CL limit, or to establish the observation of the Higgs boson at the  $3\sigma$  or  $5\sigma$  level are displayed in Figure 2a. Evidently, large integrated luminosities ( $10$  to  $30 \text{ fb}^{-1}$ ) are needed to reach a definite conclusion on the observation of the Higgs boson at the Tevatron.

Production rates for the Higgs boson in the Standard Model are significantly larger at the LHC. The dominant Higgs production process, gluon fusion, can be exploited in conjunction with a variety of other channels, *e.g.*,  $WW/ZZ$  fusion of the Higgs boson and Higgs radiation off top quarks [31, 32, 33]. Integrated luminosities between  $30$  and  $100 \text{ fb}^{-1}$ , achievable within the first few years of LHC operation, will be sufficient to cover the entire canonical Higgs mass range of the Standard Model up to values close to  $1 \text{ TeV}$  with a significance greater than  $5\sigma$  as shown in Figure 2b. Thus, there is no escape route for the SM Higgs boson at the LHC.

If a SM Higgs boson is discovered at the Tevatron, the Higgs mass can be measured with an accuracy of order  $2 \text{ GeV}$  [34], whereas the determination of Higgs couplings to  $W$  and  $Z$  bosons and to bottom quarks will be model-dependent and fairly crude. More precise measurements of the properties of the Higgs boson mass in the Standard Model can be performed at the LHC. The  $h_{\text{SM}} \rightarrow ZZ^{(*)} \rightarrow \ell^+\ell^-\ell^+\ell^-$  channel allows for an accurate Higgs mass determination of about  $0.1\%$  for  $120 \text{ GeV} \lesssim m_{h_{\text{SM}}} \lesssim 400 \text{ GeV}$ , assuming an integrated luminosity of  $300 \text{ fb}^{-1}$  [35]. For larger Higgs masses, the precision in the Higgs mass measurement deteriorates due to the effect of the increasing Higgs width; nevertheless a  $1\%$  Higgs mass measurement is possible for  $m_{h_{\text{SM}}} \simeq 700 \text{ GeV}$ . The Higgs width can be extracted with a precision of  $5$  to  $6\%$  over the mass range  $300$ — $700 \text{ GeV}$  from the Breit-Wigner shape of the Higgs resonance [35]. Below  $300 \text{ GeV}$ , the instrumental resolution becomes larger than the Higgs width, and the accuracy of the Higgs width measurement degrades. For example, the four-lepton

invariant mass spectrum from  $h_{\text{SM}} \rightarrow ZZ$  yields a precision of about 25% at  $m_{h_{\text{SM}}} = 240$  GeV [34]. For lower Higgs masses, indirect methods must be employed to measure the Higgs width.

For Higgs masses below 200 GeV, a number of different Higgs decay channels can be studied at the LHC. The relevant processes are [32, 36]:

$$\begin{aligned} gg &\rightarrow h_{\text{SM}} \rightarrow \gamma\gamma, \\ gg &\rightarrow h_{\text{SM}} \rightarrow VV^{(*)}, \\ qq &\rightarrow qqV^{(*)}V^{(*)} \rightarrow qqh_{\text{SM}}, \quad h_{\text{SM}} \rightarrow \gamma\gamma, \tau^+\tau^-, VV^{(*)}, \\ gg, q\bar{q} &\rightarrow t\bar{t}h_{\text{SM}}, \quad h_{\text{SM}} \rightarrow b\bar{b}, \gamma\gamma, WW^{(*)}, \end{aligned}$$

where  $V = W$  or  $Z$ . The gluon-gluon fusion mechanism is the dominant Higgs production mechanism at the LHC, yielding a total cross section of about 30 pb [15 pb] for  $m_{h_{\text{SM}}} = 120$  GeV [ $m_{h_{\text{SM}}} = 200$  GeV]. One also has appreciable Higgs production via  $VV$  electroweak gauge boson fusion, with a total cross section of about 6 pb [3 pb] for the Higgs masses quoted above. The electroweak gauge boson fusion mechanism can be separated from the gluon fusion process by employing a forward jet tag and central jet vetoing techniques. The cross section for  $t\bar{t}h_{\text{SM}}$  production can be significant for Higgs masses in the intermediate mass range [37], 0.8 pb [0.2 pb] at  $m_{h_{\text{SM}}} = 120$  GeV [ $m_{h_{\text{SM}}} = 200$  GeV], although this cross section falls faster with Higgs mass as compared to the gluon and gauge boson fusion mechanisms.

The measurements of various relations between Higgs decay branching ratios can be used to infer the ratios of various Higgs couplings, and provide an important first step in clarifying the nature of the Higgs boson. These can be extracted from a variety of Higgs signals which are observable over a limited range of Higgs masses. In the mass range  $110 \text{ GeV} \lesssim m_{h_{\text{SM}}} \lesssim 150 \text{ GeV}$ , the Higgs boson can be detected [with  $100 \text{ fb}^{-1}$  of data] in the  $\gamma\gamma$  and the  $\tau^+\tau^-$  channels indicated above. For  $m_{h_{\text{SM}}} \gtrsim 130$  GeV, the Higgs boson can also be detected in gluon-gluon fusion through its decay to  $WW^{(*)}$ , with both final gauge bosons decaying leptonically [38], and to  $ZZ^{(*)}$  in the four-lepton decay mode [31, 32]. There is additional sensitivity to Higgs production via  $VV$  fusion followed by its decay to  $WW^{(*)}$  for  $m_{h_{\text{SM}}} \gtrsim 120$  GeV. These data can be used to extract the ratios of the Higgs partial widths to gluon pairs, photon pairs,  $\tau^+\tau^-$ , and  $W^+W^-$  [39, 40]. The expected accuracies in Higgs width ratios, partial widths, and the total Higgs width are exhibited in Figure 3. These results are obtained under the assumption that the partial Higgs widths to  $W^+W^-$  and  $ZZ$  are fixed by electroweak gauge invariance, and the ratio of the partial Higgs widths to  $b\bar{b}$  and  $\tau^+\tau^-$  are fixed by the universality of Higgs couplings to down-type fermions. One can then extract the total Higgs width under the assumption that all other unobserved modes, in the Standard Model and beyond, possess small branching ratios of order 1%. Finally, we note that the specific Lorentz structure predicted for the  $h_{\text{SM}}W^+W^-$  coupling by the Higgs mechanism can be tested in angular correlations between the spectator jets in  $WW$  fusion of the Higgs boson at the LHC [40].

With an integrated luminosity of  $100 \text{ fb}^{-1}$  per experiment, the relative accuracy expected at the LHC for various ratios of Higgs partial widths  $\Gamma_i$  range from 10% to 30%, as shown in Figure 3. These correspond to 5% to 15% measurements of various ratios of Higgs couplings. The ratio  $\Gamma_\tau/\Gamma_W$  measures the coupling of down-type fermions relative to the Higgs couplings to gauge bosons. To the extent that the one-loop  $h_{\text{SM}}\gamma\gamma$  amplitude is dominated by the  $W$ -loop, the partial width ratio  $\Gamma_\tau/\Gamma_\gamma$  probes the same relationship. In contrast, under the usual assumption that the one-loop  $h_{\text{SM}}gg$  amplitude is dominated by the top-quark loop, the ratio  $\Gamma_g/\Gamma_W$  probes the coupling of up-type fermions relative to the  $h_{\text{SM}}WW$  coupling. Additional information about Higgs couplings can be ascertained by making use of the  $t\bar{t}h_{\text{SM}}$  production mode at the LHC, followed by  $h_{\text{SM}} \rightarrow b\bar{b}$ . Recent studies [41, 42] by the ATLAS and CMS collaborations suggest that for an integrated luminosity of

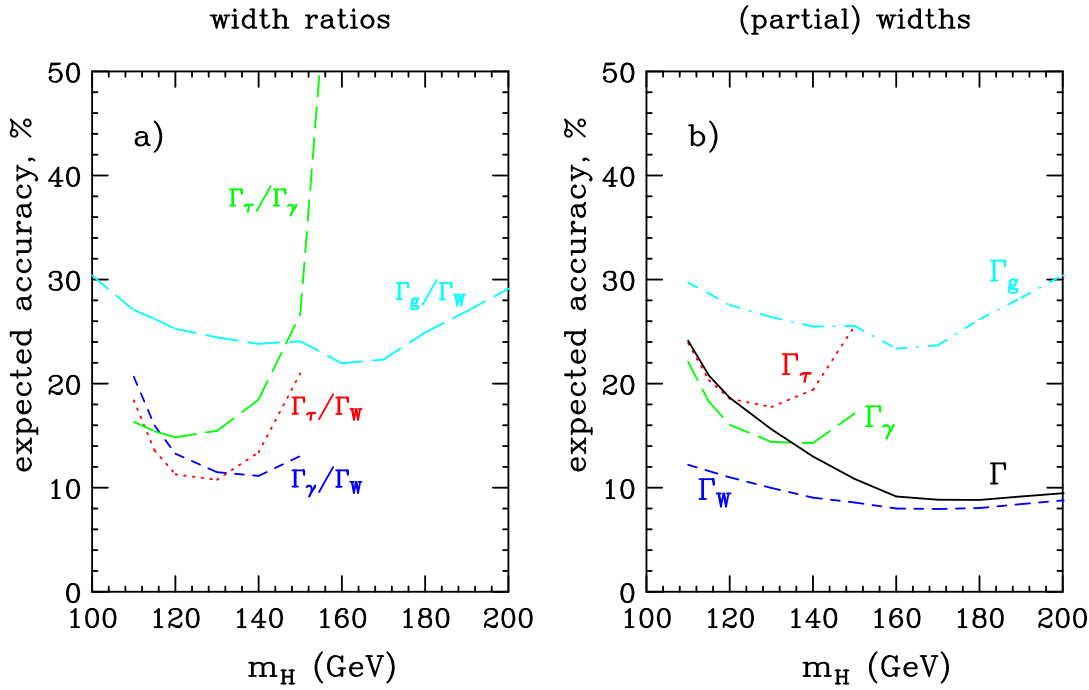


FIG. 3: Relative accuracy expected at the LHC with  $200 \text{ fb}^{-1}$  of data for (a) various ratios of Higgs boson partial widths and (b) the indirect determination of partial and total widths. Expectations for width ratios assume  $W, Z$  universality; indirect width measurements also assume  $b, \tau$  universality and a small branching ratio for unobserved modes. Taken from the parton-level analysis of Ref. [39].

100  $\text{fb}^{-1}$ , this signal is viable if  $m_{h_{\text{SM}}} \lesssim 130 \text{ GeV}$ . Including the  $t\bar{t}h_{\text{SM}}$  mode allows for an independent check of the Higgs-top quark Yukawa coupling. Moreover, if combined with information obtained from  $\Gamma_g$ , one can test, through the decay  $h_{\text{SM}} \rightarrow b\bar{b}$ , the assumption of universality of Higgs couplings to down-type fermions.

Finally, one can check the consistency of the Standard Model by comparing the observed Higgs mass to the value deduced from precision electroweak fits. With improvements expected both for the precision in the measured values of  $m_W$ ,  $m_t$  and the electroweak mixing angle, one can anticipate an improvement in the fractional  $1\sigma$  uncertainty in the Higgs mass at future colliders [43]. After  $2 \text{ fb}^{-1}$  [ $15 \text{ fb}^{-1}$ ] of integrated luminosity at the Tevatron, the anticipated fractional Higgs mass uncertainty will decrease to about 35% [25%]. Further improvements at the LHC with  $100 \text{ fb}^{-1}$  of data can reduce this uncertainty to about 18%. This will yield strong constraints on the Standard Model and could provide evidence for new physics if a disagreement is found between the inferred Higgs mass from precision measurements and the actual Higgs mass, or if no Higgs boson is discovered.

### B. Higgs Bosons in Supersymmetric Extensions of the Standard Model

In supersymmetric extensions of the Standard Model, there is one neutral Higgs state which often exhibits properties similar to those of the SM Higgs boson. In addition, new neutral and charged scalar states arise whose properties encode the physics of the electroweak symmetry breaking dynamics. In the absence of CP violation, the neutral Higgs bosons carry definite CP quantum numbers.

In the minimal supersymmetric extension of the Standard Model (MSSM), the tree-level Higgs sector is

automatically CP conserving. CP-violating effects can enter via loop corrections, and can be significant in certain regions of MSSM parameter space. However, unless otherwise noted, we will neglect CP-violating Higgs sector effects in what follows. The mass of the lightest CP-even neutral Higgs boson ( $h$ ) of the MSSM is less than about 135 GeV [8]. This prediction incorporates significant radiative corrections, which shift the maximal Higgs mass from its tree-level value of  $m_Z$  [44]. This maximal mass is achieved when the top-squark mixing parameters are such that the contribution from the radiative corrections associated with loops of top-squarks is maximal (this is the *maximal mixing* scenario). In addition, the Higgs spectrum contains a heavier CP-even neutral Higgs boson ( $H$ ), a CP-odd neutral Higgs boson ( $A$ ) and a charged Higgs pair ( $H^\pm$ ). In contrast to the  $h$  mass, the masses of the  $H$ ,  $A$  and  $H^\pm$  Higgs bosons are not similarly constrained and can be significantly larger than the  $Z$  mass. In the MSSM, the tree-level Higgs sector is fixed by the values of  $m_A$  and the ratio of Higgs vacuum expectation values,  $\tan \beta$ . When radiative corrections are included, additional MSSM parameters enter and determine the size of the loop corrections. For example, in the maximal mixing scenario (with other MSSM parameters specified according to Table 53 of Ref. [28]), most of the  $m_A$ – $\tan \beta$  parameter space can be covered at the Tevatron given sufficient luminosity [shaded areas in Figure 4a] by the search for CP-even Higgs bosons with significant couplings to the  $W$  and  $Z$ . The remaining unexplored regions will be covered at the LHC [Figure 4b]. That is, at least one of the Higgs bosons of the MSSM is guaranteed to be discovered at either the Tevatron and/or the LHC. The coverage in the  $m_A$ – $\tan \beta$  plane by different Higgs production and decay channels can vary significantly, depending on the choice of MSSM parameters. For example, if the CP-even

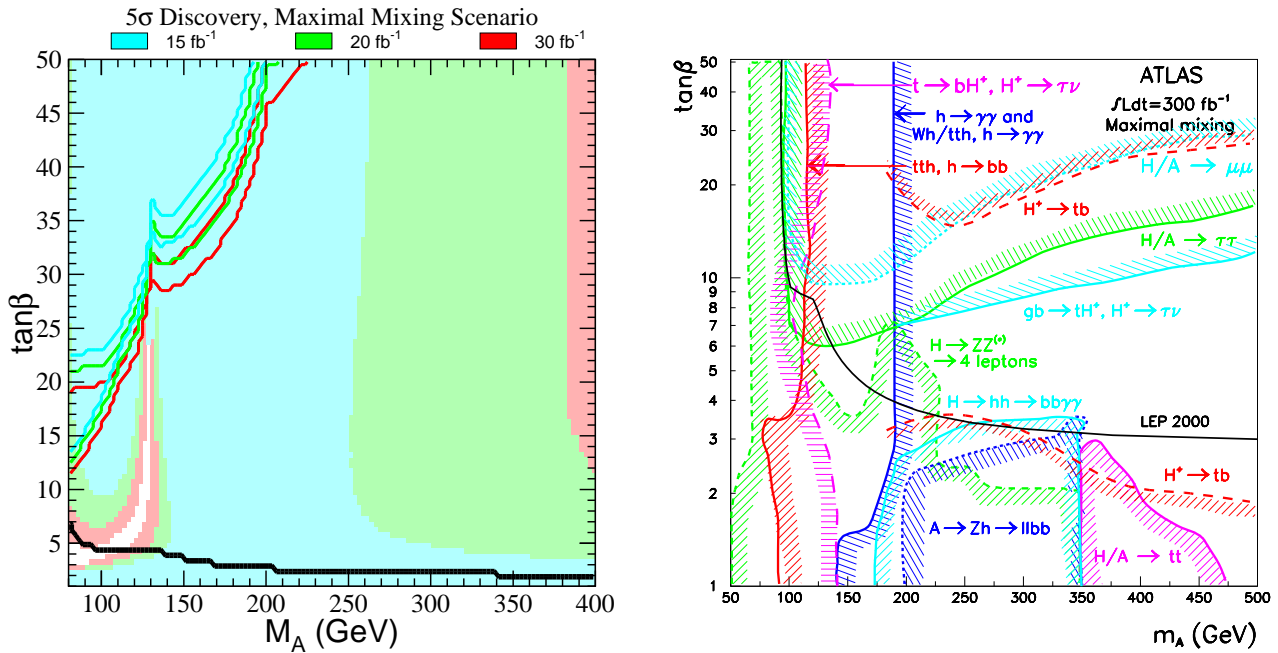


FIG. 4: (a)  $5\sigma$  discovery region on the  $m_A$ – $\tan \beta$  plane [28], for the maximal mixing scenario and two different search channels:  $q\bar{q} \rightarrow V\phi$  ( $\phi = h, H$ ),  $\phi \rightarrow b\bar{b}$  (shaded regions) and  $gg$ ,  $q\bar{q} \rightarrow b\bar{b}\phi$  ( $\phi = h, H, A$ ),  $\phi \rightarrow b\bar{b}$  (region in the upper left-hand corner bounded by the solid lines). Different integrated luminosities are explicitly shown by the color coding. The two sets of lines (for a given color) correspond to the CDF and DØ simulations, respectively. The region below the solid black line near the bottom of the plot is excluded by the absence of observed  $e^+e^- \rightarrow Z\phi$  events at LEP2. (b)  $5\sigma$  discovery contours for MSSM Higgs boson detection in various channels are shown in the  $m_A$ – $\tan \beta$  parameter space, in the maximal mixing scenario, assuming an integrated luminosity of  $L = 300 \text{ fb}^{-1}$  for the ATLAS detector [31, 32].

Higgs boson with the larger coupling to the  $W$  and  $Z$  has a strongly suppressed coupling to bottom quarks, the Higgs searches at the Tevatron will become more problematical, while the LHC search for Higgs production followed by its decay into photons becomes more favorable [45].

In some regions of MSSM parameter space, more than one Higgs boson can be discovered at the LHC. However, there is a sizable wedge-shaped region of the parameter space at moderate values of  $\tan\beta$  opening up from about  $m_A = 200$  GeV to higher values in which the heavier Higgs bosons cannot be discovered at the LHC [see Figure 4b]. In this region of the MSSM parameter space, only the lightest CP-even Higgs boson can be discovered, and its properties are nearly indistinguishable from those of the SM Higgs boson. Deviations from SM properties can also occur if the Higgs decay into supersymmetric particles is kinematically allowed, or if light supersymmetric particles contribute significantly to Higgs loop amplitudes. High precision measurements of Higgs branching ratios and other properties will be required in order to detect deviations from SM Higgs predictions and demonstrate the existence of a non-minimal Higgs sector.

The phenomenology of the MSSM Higgs sector is closely tied to various MSSM parameters that arise as a consequence of low-energy supersymmetry breaking. *A priori*, one can parameterize this breaking in terms of the most general set of soft supersymmetry-breaking terms [46]. Alternatively, one can propose models of fundamental supersymmetry breaking, which constrain many of these terms. The *Snowmass points and slopes (SPS)*, developed in Ref. [47], are a consensus of benchmark points and model lines (“slopes”) within various theoretical approaches to supersymmetry breaking, which correspond to different scenarios in the search for supersymmetry at future colliders. One expects a significant interplay between the study of supersymmetric phenomena and the observation of Higgs bosons and their properties. Ultimately, one hopes to learn if (and how) the origin of electroweak breaking depends fundamentally on the physics of supersymmetry breaking.

### C. Strong Electroweak Symmetry Breaking Dynamics

If strong electroweak symmetry breaking with no Higgs boson in the mass range below 1 TeV is realized in nature, the Tevatron may provide the first hints of new physics, while LHC can provide some insight into the domain of the new strong interactions [48]. The top quark may play a critical role in this enterprise, due to the fact that its large mass implies the strongest coupling to the electroweak symmetry breaking sector, compared to the other known particles of the Standard Model. At the Tevatron, hints of new physics associated with the top quark can emerge in a number of ways. Anomalous top quark production and/or new particles that decay into  $t\bar{t}$  pairs would be a possible signal of strong electroweak symmetry-breaking dynamics.

At the LHC, deviations from the perturbative predictions for  $W^+W^-$  production in quark-antiquark collisions shed light on the onset of the new interactions between the  $W$  bosons below 3 TeV. This range is also expected to be covered in strong  $WW$  quasi-elastic scattering. Access to this new domain can also be provided by observing pseudo-Goldstone bosons associated with the spontaneous breaking of global symmetries of the new strong interactions [49]. In addition, the observation of genuine new resonances (made up of techniquarks or other new fundamental strongly-interacting particles) is possible for masses below 2 to 3 TeV [32]. Evidence for new substructure can also be detected indirectly via deviations in jet-jet and Drell-Yan cross sections. For example, with  $300 \text{ fb}^{-1}$  of data, the measurement of the dijet cross section is sensitive to a compositeness scale of about 40 TeV. However, the energy of the LHC and the resolution of the experiments fall short of a detailed analysis of the new strong interactions.

### III. EWSB PHYSICS AT FUTURE $e^+e^-$ LINEAR COLLIDERS

#### A. Standard Model Higgs Boson

The next generation of high energy  $e^+e^-$  linear colliders is expected to operate at energies from 300 GeV up to about 1 TeV (JLC, NLC, TESLA), henceforth referred to as the LC [50, 51, 52]. The possibility of a multi-TeV linear collider operating in an energy range of 3–5 TeV (CLIC) is also under study [53]. With the expected high luminosities, up to  $1 \text{ ab}^{-1}$ , accumulated within a few years in a clean experimental environment, these colliders are ideal instruments for reconstructing the mechanism of electroweak symmetry breaking in a comprehensive and conclusive form.

If weakly-coupled electroweak symmetry breaking dynamics (involving an elementary scalar Higgs field) is realized in nature, then it can be established experimentally in three steps:

1. The Higgs boson must be observed clearly and unambiguously, and its basic properties—mass, width, spin and C and P quantum numbers—must be determined.
2. The couplings of the Higgs boson to the  $W^\pm$  and  $Z$  bosons and to leptons and quarks must be measured. Demonstrating that these couplings scale with the mass of the corresponding particle would provide a critical verification of the Higgs mechanism as the responsible agent for generating the masses of the fundamental particles.
3. The Higgs potential must be reconstructed by measuring the self-coupling of the Higgs field. The specific form of the potential shifts the ground state to a non-zero value, thereby providing the mechanism for electroweak symmetry breaking based on the self-interactions of scalar fields.

Essential elements of this program can be realized at a high-luminosity  $e^+e^-$  linear collider [54, 55, 56]. With an accumulated luminosity of  $500 \text{ fb}^{-1}$ , about  $10^5$  Higgs bosons can be produced by Higgs-strahlung  $e^+e^- \rightarrow Zh_{\text{SM}}$  in the theoretically preferred intermediate mass range below 200 GeV. Given the low background, as illustrated in Figure 5a [57], high-precision analyses of the Higgs boson are possible in these machines. The Higgs mass will be measured to an accuracy of order 100 MeV (with an achievable fractional precision of  $5 \times 10^{-4}$  for  $m_{h_{\text{SM}}} = 120 \text{ GeV}$ ). The Higgs width can be inferred, in a model-independent way, to an accuracy up to 5 %, by combining the partial width to  $W^+W^-$ , accessible in the vector boson fusion process, with the  $W^+W^-$  decay branching ratio. Spin and parity can be determined unambiguously from the steep onset of the excitation curve in Higgs-strahlung near the threshold (see Figure 5b [58]) and the angular correlations in this process.

Higgs decay branching ratios can be measured very precisely in the intermediate mass range (as shown in Figure 5c [59]). When these measurements are combined with measurements of Higgs production cross sections, the absolute values of the Higgs couplings to the  $W^\pm$  and  $Z$  gauge bosons and the Yukawa couplings to leptons and quarks can be determined to a few percent in a model-independent way. In addition, the Higgs-top Yukawa coupling can be inferred from the cross section for Higgs emission off top-antitop quark pairs [60, 61]. The expected accuracies for the measurements of Higgs couplings is given in Table I. These observations are essential for establishing weakly-coupled scalar dynamics and the associated Yukawa interactions as the mechanism generating the masses of the fundamental particles in the Standard Model.

The measurement of the self-couplings of the Higgs field is a very ambitious task that requires the highest luminosities possible at  $e^+e^-$  linear colliders, which possess unique capabilities for addressing this question. The trilinear Higgs self-coupling can be measured in double Higgs-strahlung, in which a virtual Higgs boson splits

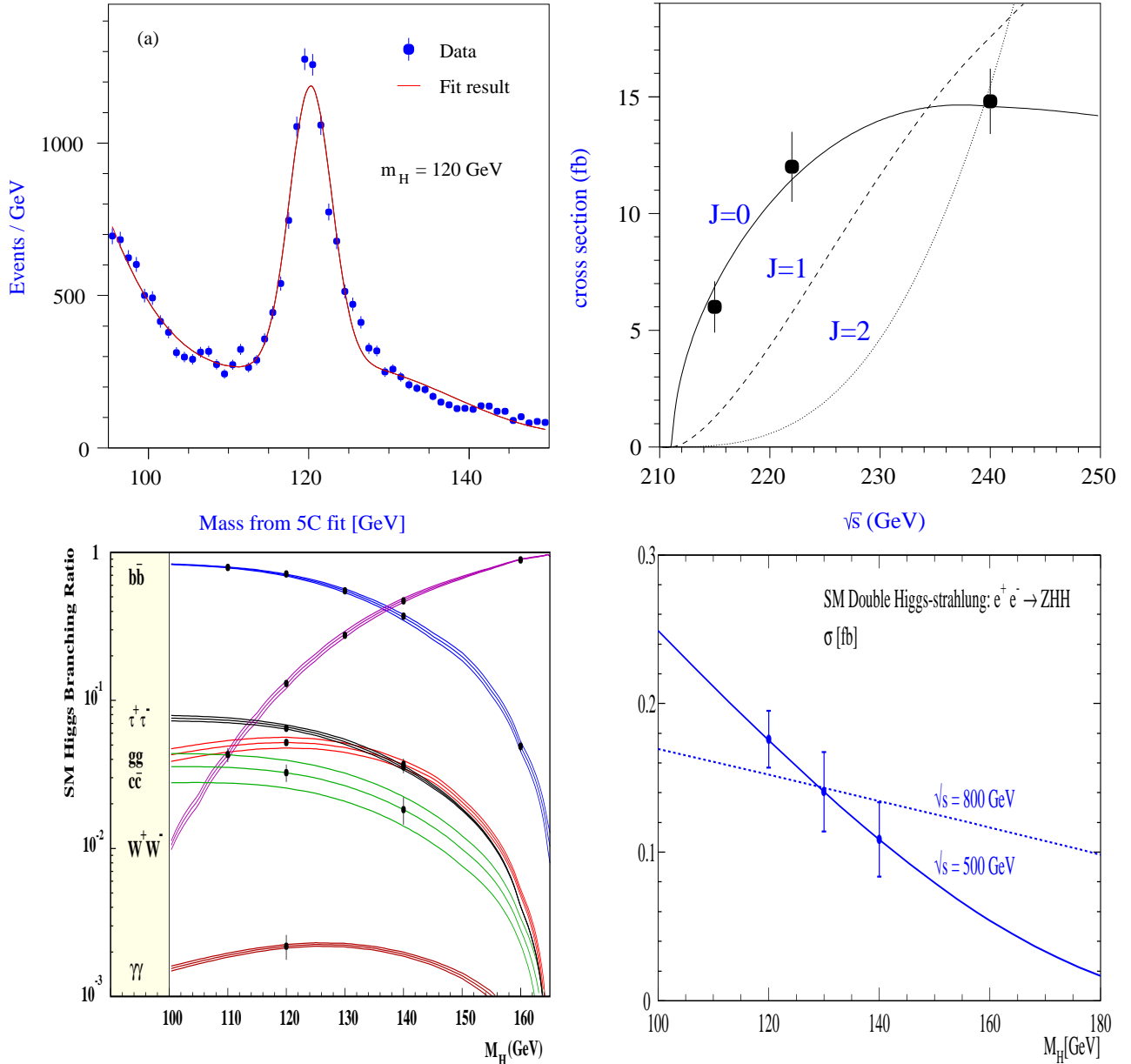


FIG. 5: (a) The Higgs boson mass peak reconstructed in the channel  $e^+e^- \rightarrow Zh_{\text{SM}} \rightarrow b\bar{b}q\bar{q}$  for  $m_{h_{\text{SM}}} = 120$  GeV [57]; (b) Simulated measurement of the  $e^+e^- \rightarrow Zh_{\text{SM}}$  cross section for  $m_{h_{\text{SM}}} = 120$  GeV with 20  $\text{fb}^{-1}$ /point at three center of mass energies compared to the predictions for spin-0 (full line) and typical examples of spin-1 particles (dashed line) and spin-2 particles (dotted line) [58]; (c) The predicted SM Higgs boson branching ratios. Points with error bars show the expected experimental accuracy, while the lines indicate the theoretical uncertainties on SM predictions [59]. (d) Cross section for the double Higgs-strahlung process  $e^+e^- \rightarrow Zh_{\text{SM}}h_{\text{SM}}$  at  $\sqrt{s} = 500$  GeV (solid line) and  $800$  GeV (dashed line) [62]. The data points show the accuracy for 1  $\text{ab}^{-1}$ .

into two real Higgs particles in the final state [62, 63]. A simulation based on 1  $\text{ab}^{-1}$  of data is exhibited in Figure 5d [62]. In this way, the cubic term of the scalar potential can be established at a precision of about 20%. Such a measurement is a prerequisite for developing the form of the Higgs potential specific for spontaneous electroweak symmetry breaking in the scalar sector.

If the SM Higgs mass is above 200 GeV, then the precision determination of Higgs couplings will have to be

Coupling	$m_{h_{\text{SM}}} = 120 \text{ GeV}$	$m_{h_{\text{SM}}} = 140 \text{ GeV}$
$h_{\text{SM}}WW$	1.3%	2.0%
$h_{\text{SM}}ZZ$	1.2%	1.3%
$h_{\text{SM}}t\bar{t}$	3.0%	6.1%
$h_{\text{SM}}b\bar{b}$	2.2%	2.2%
$h_{\text{SM}}c\bar{c}$	3.7%	10.2%
$h_{\text{SM}}\tau\tau$	3.3%	4.8%

TABLE I: Expected accuracies for measurements of Higgs couplings at an  $e^+e^-$  linear collider for Higgs masses of 120 and 140 GeV in the Standard Model, from Ref. [59]. For the  $WW$  and  $ZZ$  couplings,  $500 \text{ fb}^{-1}$  at  $\sqrt{s} = 500 \text{ GeV}$  are assumed. For  $b\bar{b}$ ,  $c\bar{c}$ , and  $\tau\tau$ , the study assumes  $500 \text{ fb}^{-1}$  at  $\sqrt{s} = 350 \text{ GeV}$ ; for  $t\bar{t}$ ,  $1 \text{ ab}^{-1}$  at  $\sqrt{s} = 800 \text{ GeV}$ .

reconsidered. The SM Higgs discovery reach at the LC is maximized by considering both the Higgs-strahlung process,  $e^+e^- \rightarrow Z h_{\text{SM}}$ , and the vector boson fusion process,  $e^+e^- \rightarrow \nu\bar{\nu}h_{\text{SM}}$ . For example, the analysis of Ref. [64] suggests that for an integrated luminosity of  $500 \text{ fb}^{-1}$ , a Higgs boson with mass up to about 650 GeV will be observable at the LC with  $\sqrt{s} = 800 \text{ GeV}$ . For Higgs masses above  $t\bar{t}$  threshold, one can measure the  $t\bar{t}h_{\text{SM}}$  Yukawa coupling by observing Higgs bosons produced by vector boson fusion which subsequently decay to  $t\bar{t}$ . The analysis of Ref. [65] finds that at the LC with  $\sqrt{s} = 800 \text{ GeV}$  and  $1 \text{ ab}^{-1}$  of data, the  $t\bar{t}h_{\text{SM}}$  Yukawa coupling can be determined with an accuracy of about 10% for a Higgs mass in the range 350—500 GeV.

The  $e^+e^-$  linear collider with center-of-mass energy  $\sqrt{s}$  can also be designed to operate in a  $\gamma\gamma$  collision mode. This is achieved by using Compton backscattered photons in the scattering of intense laser photons on the initial polarized  $e^\pm$  beams [66, 67]. The resulting  $\gamma\gamma$  center of mass energy is peaked for proper choices of machine parameters at about  $0.8\sqrt{s}$ . The luminosity achievable as a function of the photon beam energy depends strongly on the machine parameters (in particular, the choice of laser polarizations). The photon collider provides additional opportunities for Higgs physics [67, 68, 69, 70, 71]. The Higgs boson can be produced as an  $s$ -channel resonance in  $\gamma\gamma$  collisions, and one can perform independent measurements of various Higgs couplings. For example, the product  $\Gamma(h_{\text{SM}} \rightarrow \gamma\gamma)\text{BR}(h_{\text{SM}} \rightarrow b\bar{b})$  can be measured with a statistical accuracy of about 2—10% for  $120 \text{ GeV} \lesssim m_{h_{\text{SM}}} \lesssim 160 \text{ GeV}$  with about  $50 \text{ fb}^{-1}$  of data [69, 70, 71]. Using values for  $\text{BR}(h_{\text{SM}} \rightarrow b\bar{b})$  and  $\text{BR}(h_{\text{SM}} \rightarrow \gamma\gamma)$  measured at the  $e^+e^-$  linear collider, one can obtain a value for the total Higgs width with an error dominated by the expected error in  $\text{BR}(h_{\text{SM}} \rightarrow \gamma\gamma)$ . For heavier Higgs bosons,  $m_{h_{\text{SM}}} \gtrsim 200 \text{ GeV}$ , the total Higgs width can in principle be measured *directly* by tuning the collider to scan across the Higgs resonance. One can also use the polarization of the photon beams to measure various asymmetries in Higgs production and decay, which are sensitive to the CP quantum number of the Higgs boson [70].

Finally, we note that substantial improvements are possible for precision measurements of  $m_W$ ,  $m_t$  and electroweak mixing angle measurements at the LC [43]. But, the most significant improvements can be achieved at the GigaZ [72], where the linear collider operates at  $\sqrt{s} = m_Z$  and  $\sqrt{s} \simeq 2m_W$ . With an integrated luminosity of  $50 \text{ fb}^{-1}$ , one can collect  $1.5 \times 10^9 Z$  events and about  $10^6 W^+W^-$  pairs in the threshold region. Employing a global fit to the precision electroweak data in the Standard Model, the anticipated fractional Higgs mass uncertainty achievable would be about 8%. This would provide a stringent test for the theory of the Higgs boson, as well as very strong constraints on any new physics beyond the Standard Model that couples to the  $W$  and  $Z$  gauge bosons.

## B. Higgs Bosons in Supersymmetric Extensions of the Standard Model

We first focus on the production of  $h$ ,  $H$ ,  $A$  and  $H^\pm$  of the MSSM. The main production mechanisms are (i) single Higgs production ( $e^+e^- \rightarrow Zh$ ,  $ZH$ ) via Higgs-strahlung, (ii) associated neutral Higgs pair production ( $e^+e^- \rightarrow hA$ ,  $HA$ ) via  $s$ -channel  $Z$  exchange, and (iii) charged Higgs pair production ( $e^+e^- \rightarrow H^+H^-$ ). Processes (i) and (ii) are complementary to each other as a consequence of unitarity sum rules for tree-level Higgs couplings [73]. In particular,  $g_{\phi ZZ}^2 + 4m_Z^2 g_{\phi AZ}^2 = g^2 m_Z^2 / \cos^2 \theta_W$  (for  $\phi = h, H$ ), which shows that both  $g_{\phi ZZ}^2$  and  $g_{\phi AZ}^2$  cannot simultaneously vanish. For  $m_A \gtrsim 200$  GeV, one finds that  $m_A \sim m_H \sim m_{H^\pm} \gg m_h$  and  $g_{HZZ} \sim g_{hAZ} \sim 0$ , as a consequence of the decoupling limit in which the properties of  $h$  are nearly indistinguishable from those of the SM Higgs boson [74]. Thus, at the LC with center-of-mass energy  $\sqrt{s}$ , the Higgs-strahlung of the lightest Higgs boson  $Zh$  and pair production of the heavy Higgs bosons  $HA$  and  $H^+H^-$  are dominant if  $m_A \lesssim \sqrt{s}/2$ . In this case, the heavy Higgs states can be cleanly reconstructed at the linear collider, as seen in Figure 6a and 6b. On the other hand, since  $m_h \lesssim 135$  GeV, a center-of-mass energy of 300 GeV is more than sufficient to cover the entire MSSM parameter space with certainty. Thus, the light Higgs boson,  $h$ , is accessible at the LC while the observation of  $H$ ,  $A$  and  $H^\pm$  is possible only if  $\sqrt{s}$  is sufficiently large. The heavier Higgs states could lie beyond the discovery reach of the LC ( $\sqrt{s} \leq 1$  TeV), and require a multi-TeV linear collider for discovery and study. In this case, the precision measurements of the light Higgs decay branching ratios and couplings achievable at an  $e^+e^-$  linear collider are critical for distinguishing between  $h_{\text{SM}}$  and  $h$  of a non-minimal Higgs sector with properties close to that of the SM Higgs boson.

To illustrate the challenge of probing the decoupling limit, suppose that  $m_A > \sqrt{s}/2$  so that only the light Higgs boson,  $h$ , can be observed directly at the LC. However, in this region of decoupling the deviation of the couplings of  $h$  from those of the SM Higgs boson approach zero. In particular, the fractional deviation scales as  $m_Z^2/m_A^2$ , so that if precision measurements reveal a non-zero deviation, one could in principle derive a constraint on the heavy Higgs masses of the model. In the MSSM, the constraint can be sensitive to the MSSM

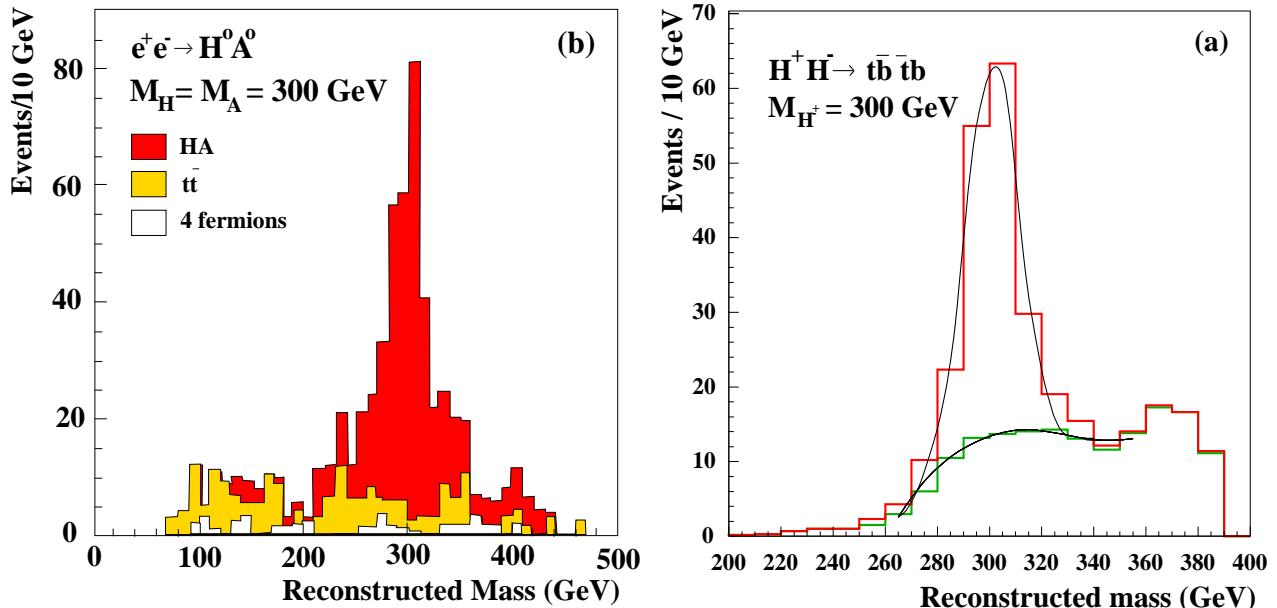


FIG. 6: Heavy MSSM Higgs states at the LC for  $\sqrt{s} = 800$  GeV [54]: (a) Reconstructed  $H$  and  $A$  mass peak from  $e^+e^- \rightarrow HA \rightarrow b\bar{b}b\bar{b}$  for  $50 \text{ fb}^{-1}$  of data; and (b) the dijet invariant mass distribution for  $e^+e^- \rightarrow H^+H^- \rightarrow t\bar{t}b\bar{b}$  candidates after applying the intermediate  $t$  and  $W$  mass and the equal final state mass constraints for  $500 \text{ fb}^{-1}$  of data.

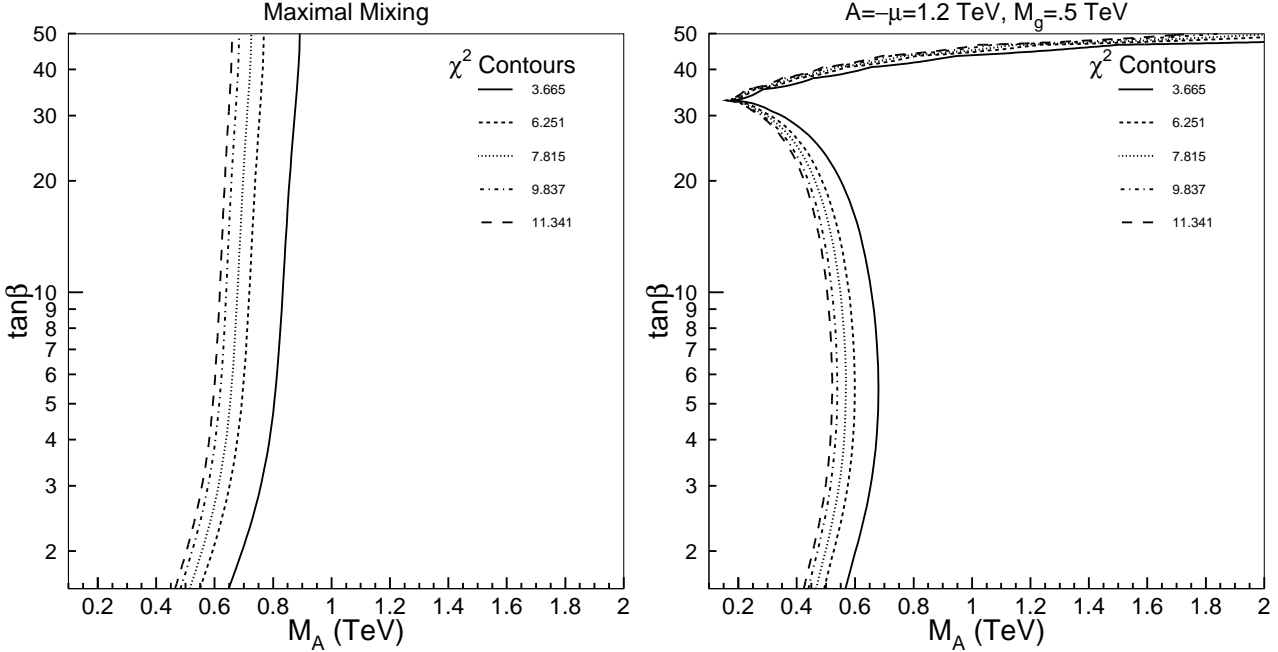


FIG. 7: Contours of  $\chi^2$  for Higgs boson decay observables for the maximal mixing scenario [left panel] and for a different choice of MSSM parameters for which the one-loop shift to the  $h\bar{b}\bar{b}$  coupling is large [right panel]. See Ref. [75] for additional details. The contours correspond to 68, 90, 95, 98 and 99% confidence levels (right to left) for the three observables  $g_{h\bar{b}\bar{b}}^2$ ,  $g_{h\tau\tau}^2$ , and  $g_{hgg}^2$ .

parameters which control the radiative corrections to the Higgs couplings. This is illustrated in Figure 7, where the constraints on  $m_A$  are derived for two different sets of MSSM parameter choices [75]. Here, a simulation of a global fit of measured  $h\bar{b}\bar{b}$ ,  $h\tau\tau$  and  $hgg$  couplings is made and  $\chi^2$  contours are plotted indicating the constraints in the  $m_A$ – $\tan\beta$  plane assuming a deviation from SM Higgs couplings is seen. In the maximal mixing scenario, the constraints on  $m_A$  are significant and rather insensitive to the value of  $\tan\beta$ . However in some cases, as shown in Figure 7b, a region of  $\tan\beta$  may yield almost no constraint on  $m_A$ . Of course, if supersymmetric particles are discovered prior to the precision Higgs measurements, additional information about the MSSM spectrum can be employed to further refine the analysis.

The  $e^+e^-$  collider running in the  $\gamma\gamma$  collider mode presents additional opportunities for the study of the MSSM Higgs sector. Resonance production  $\gamma\gamma \rightarrow H$  and  $A$  can be used to extend the reach in Higgs masses beyond the limit set by  $HA$  pair production in the  $e^+e^-$  mode [70, 71, 76]. Typically, one can probe the heavy Higgs masses out to  $m_A \sim 0.8\sqrt{s}$  (where  $\sqrt{s}$  is the center of mass energy of the LC). This extends the MSSM Higgs search to regions of the  $m_A$ – $\tan\beta$  parameter space for which the LHC is not sensitive in general (the so-called “blind wedge” of large  $m_A$  and moderate values of  $\tan\beta$ ).

As noted above, at least one Higgs boson must be observable at the LC in the MSSM. In non-minimal supersymmetric models, additional Higgs bosons appear in the spectrum, and the “no-lose” theorem of the MSSM must be reconsidered. For example, in the non-minimal supersymmetric extension of the Standard Model (the so-called NMSSM where a Higgs singlet is added to the model [77]), the lightest Higgs boson decouples from the  $Z$  boson if its wave function is dominated by the Higgs singlet component. However, in this case the second lightest Higgs boson usually plays the role of  $h$  of the MSSM. That is, the mass of the second

lightest neutral CP-even Higgs boson is light (typically below 150 GeV) with significant couplings to the  $Z$ , so that it can be produced by the Higgs-strahlung process with an observable cross section [78]. If the second lightest Higgs boson also decouples from the  $Z$ , then the third lightest will play the role of the lightest CP-even Higgs boson of the MSSM for which the observation is ensured, and so on. Even in bizarre scenarios where all the neutral Higgs boson share equally in the coupling to  $ZZ$  (with the sum of all squared couplings constrained to equal the square of the  $h_{\text{SM}}ZZ$  coupling [73]), the “no-lose” theorem still applies—Higgs production at the LC must be observable [79]. In contrast, despite significant progress, there is no complete guarantee that at least one Higgs boson of the NMSSM must be discovered at the LHC for all choices of the model parameters [80].

One of the key parameters of the MSSM Higgs sector is the value of the ratio of Higgs vacuum expectation values,  $\tan\beta$ . In addition to providing information about the structure of the non-minimal Higgs sector, the measurement of this parameter also provides an important check of supersymmetric structure, since this parameter also enters the chargino, neutralino and third generation squark mass matrices and couplings. Thus,  $\tan\beta$  can be measured independently using supersymmetric processes and compared to the value obtained from studying the Higgs sector. Near the decoupling limit, the properties of  $h$  are almost indistinguishable from those of  $h_{\text{SM}}$ , and thus no information can be extracted on the value of  $\tan\beta$ . However, the properties of the heavier Higgs bosons are  $\tan\beta$ -dependent. Far from the decoupling limit, all Higgs bosons of the MSSM will be observable at the LC and exhibit strong  $\tan\beta$ -dependence in their couplings. Thus, to extract a value of  $\tan\beta$  from Higgs processes, one must observe the effects of the heavier Higgs bosons of the MSSM at the LC.

The ultimate accuracy of the  $\tan\beta$  measurement at the LC depends on the value of  $\tan\beta$ . In Ref. [81], it is argued that one must use a number of processes, including  $b\bar{b}b\bar{b}$  final states arising from  $b\bar{b}H$ ,  $b\bar{b}A$ , and  $HA$  production, and  $t\bar{t}b\bar{b}$  final states arising from  $t\bar{b}H^+$ ,  $b\bar{t}H^-$  and  $H^+H^-$  production. One subtlety that arises here is that in certain processes, the determination of  $\tan\beta$  may be sensitive to loop corrections that depend on the values of other supersymmetric parameters. One must settle on a consistent definition of  $\tan\beta$  when loop corrections are included [analogous to the ambiguity in the definition of the one-loop electroweak mixing angle]. A comprehensive analysis of the extraction of  $\tan\beta$  from collider data, which incorporates loop effects, has not yet been given.

The study of the properties of the heavier MSSM Higgs bosons (mass, width, branching ratios, quantum numbers, *etc.*) provides a number of additional challenges. For example, in the absence of CP-violation, the heavy CP-even and CP-odd Higgs bosons,  $H$  and  $A$ , are expected to be nearly mass-degenerate. Their CP quantum numbers and their separation can be investigated at the same time in the photon-photon collider mode of the LC. If linearly polarized photons are used in parallel polarization states, only the CP-even Higgs boson  $H$  will be produced, while in perpendicular polarization states only the CP-odd Higgs boson  $A$  will be produced. Thus, the CP quantum numbers and the separation of the two different states can be achieved. So far, we have implicitly assumed that the neutral Higgs bosons are CP eigenstates. In the MSSM, the Higgs-sector is CP-conserving at tree-level. But, in supersymmetric models with explicit CP violation, radiative corrections can induce nontrivial CP-mixing among the neutral Higgs states [82]. In the decoupling limit, the lightest Higgs boson,  $h$ , remains CP-even, while the two heavier Higgs states mix and exhibit CP-violating interactions with fermions [83]. In non-minimal supersymmetric extensions of the Standard Model, the more complicated Higgs sectors can also exhibit CP-violating properties. In the case of a CP-violating Higgs sector, the observation and measurement of the Higgs bosons become much more challenging, and an  $e^+e^-$  collider can uniquely test the nature of the couplings of the Higgs neutral eigenstates of mixed CP parity to gauge bosons and fermions.

### C. Strong Electroweak Symmetry Breaking Dynamics

Important steps in exploring strong electroweak symmetry breaking can be taken already at the LC with  $\sqrt{s} \geq 500$  GeV and an integrated luminosity of  $500 \text{ fb}^{-1}$  and above. Even if the masses of new heavy resonances associated with the symmetry breaking sector are in the TeV range, their effects can be indirectly observed at the LC with  $\sqrt{s} \leq 1$  TeV. In  $e^+e^- \rightarrow W^+W^-$ , the entire threshold region for the onset of the new strong interactions can be covered up to scales of 3 TeV [84]. Strong quasi-elastic  $WW$  scattering, the  $W$  bosons emitted from the high-energy electron and positron beams, can be studied directly up to scales of the same size [85]. Isospin-zero resonance channels as well as isospin-two exotic channels are accessible in this way. New  $\rho$ -type resonances can be studied as virtual states for masses up to several TeV, as illustrated in Figure 8. Pseudo-Goldstone bosons may be accessible in  $e^+e^-$  annihilation and  $\gamma\gamma$  collisions up to a few hundred GeV [49, 86].

Strong gauge boson interactions also can induce anomalous triple and quartic gauge couplings at tree-level. Both CP-conserving and CP-violating couplings are possible. For example, precision measurements of the process  $e^+e^- \rightarrow W^+W^-$  are sensitive to anomalous contributions to the static magnetic and electric dipole and quadrupole moments. The expected errors in the anomalous couplings, relative to the Standard Model triple gauge boson coupling, range from  $10^{-4}$  to  $10^{-3}$  at the LC with  $\sqrt{s} = 500$  GeV to 1 TeV and an integrated luminosity of 0.5 to 1  $\text{ab}^{-1}$ . At these accuracies, one can begin to probe the contributions to the anomalous couplings from Standard Model (or MSSM) perturbative one-loop corrections. Corrections due to the strong electroweak symmetry breaking sector are likely to be of the same order of magnitude, or perhaps somewhat larger, and they can provide independent evidence for the existence of new TeV-scale physics.

A multi-TeV  $e^+e^-$  collider is an excellent tool to study new strong interaction resonances in great detail. Since  $W$  bosons can be reconstructed in the jet decay channels, the dynamics of the new resonances can be explored in a more comprehensive way than at hadron colliders. Such a machine is the appropriate instrument for fully developing the picture of the new strong forces in the electroweak sector.

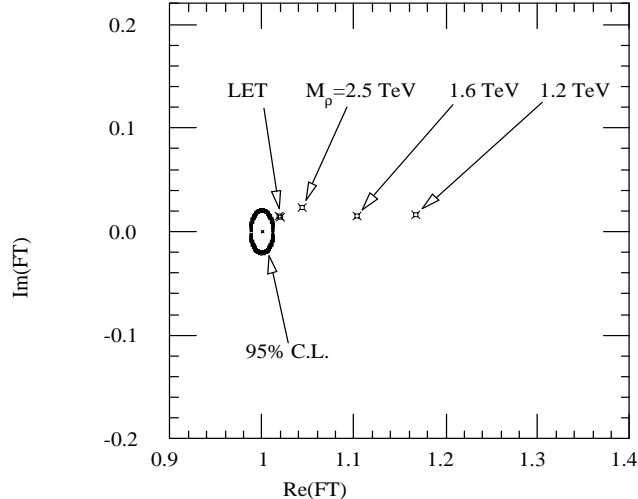


FIG. 8: The  $W_L W_L$  scattering form factor  $F_T$ , for various masses  $M_\rho$  of a new vector resonance in  $e^+e^- \rightarrow W^+W^-$ . The strong threshold effects in  $WW$  scattering, based on taking the  $WW$  amplitude to be exactly given by the amplitude as predicted by the low-energy theorem (LET), is indicated by the LET point. The contour is indicative for the precision attainable with  $500 \text{ fb}^{-1}$  at  $\sqrt{s} = 500$  GeV. Taken from [84].

## IV. EWSB PHYSICS AT FAR-FUTURE COLLIDER FACILITIES

### A. Probing EWSB at a $\mu^+\mu^-$ Collider

In contrast to Higgs production at electron-positron colliders, the Higgs boson can be produced as an  $s$ -channel resonance in a  $\mu^+\mu^-$  collider [87, 88, 89, 90, 91, 92] with an appreciable rate, since the Higgs coupling to muons is sufficiently large to generate a sizeable production cross section. For a Higgs boson mass in the lower part of the intermediate mass range, roughly  $10^4$  particles can be produced in a few years, with the same number of background events in the  $b\bar{b}$  channel. Given the expected energy resolution, the Higgs mass can be measured in such a machine with the accuracy of a few MeV, as shown in Figure 9a, similar to the precision of the  $Z$  mass measurement at LEP. The Higgs width can be measured directly from a scan of the Higgs lineshape, with an accuracy of order 20%. Since the Higgs-boson width becomes rapidly wider at the upper end of the intermediate mass range, the Higgs resonance-signal is no longer observable at the  $\mu^+\mu^-$  collider for  $m_{h_{\text{SM}}} \gtrsim 160$  to 180 GeV. Anticipating the discovery of a fundamental relation between the Higgs mass and the  $Z$  mass in a future comprehensive theory of particle physics, the high precision with which the Higgs boson mass can be measured at a muon collider could turn out to be a critical aspect in testing such a theory, in analogy to the relation between the  $Z, W^\pm$  masses and the electroweak mixing angle in the Standard Model.

The sharp energy of a muon collider can be exploited to resolve the nearly mass-degenerate CP-even Higgs boson  $H$  and the CP-odd Higgs boson  $A$  in supersymmetric theories, as shown in Figure 9b. Clearly, many other aspects of the Higgs sector can be studied at a  $\mu^+\mu^-$  collider [87, 92]. In particular, if polarized beams are available, one could explore the CP quantum numbers of the Higgs boson(s) or probe CP-violation in the Higgs sector. There are several CP-violating observables, which are unique to  $s$ -channel Higgs production at the  $\mu^+\mu^-$  collider, that can be constructed using muon polarization vectors [87, 93] and/or three-momenta and

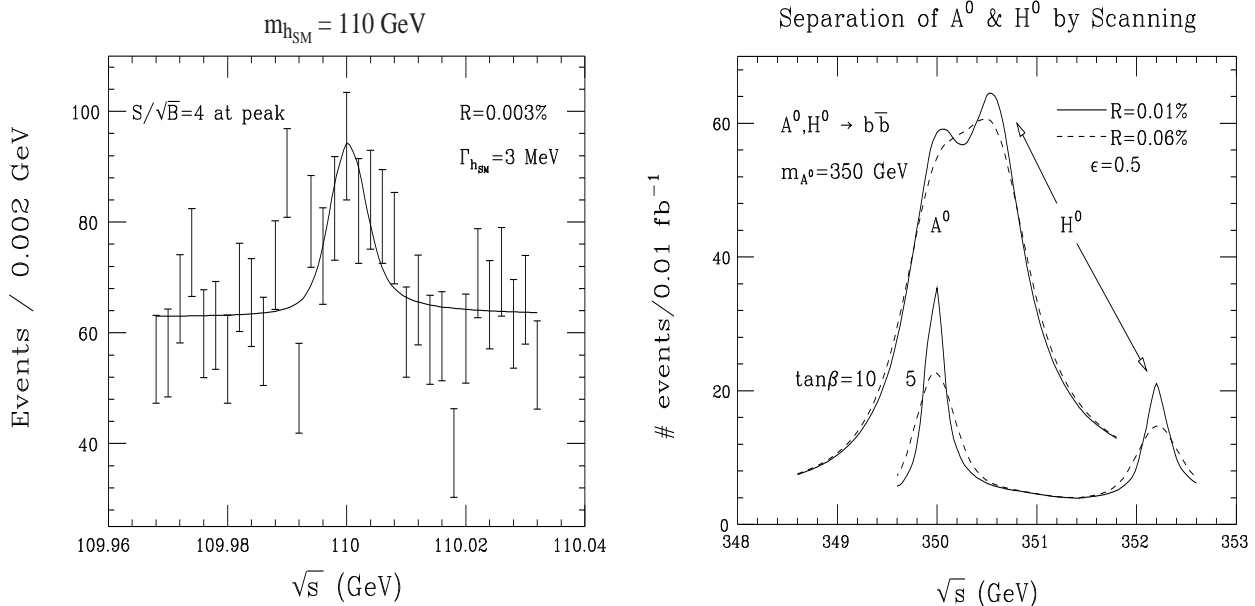


FIG. 9: Higgs-boson signals at a muon collider, taken from Refs. [88] and [87]. (a) Scan of the  $s$ -channel Higgs resonance in the Standard Model for  $m_{h_{\text{SM}}} = 110$  GeV assuming a beam energy width of  $R = 0.003\%$  and  $1.5 \text{ pb}^{-1}$  per scan point. (b) Resolution of  $H-A$  splitting in supersymmetric theories.

spins of the final particles [94]. These asymmetries are degraded for partially polarized muon beams and by the effects of the precession of the spins of the colliding beams. Nevertheless, in some cases, the CP quantum number of the SM Higgs boson or of the neutral Higgs bosons of an extended Higgs sector can be extracted with reasonable accuracy [92, 95] (e.g., for the MSSM Higgs sector with large radiatively-induced CP-violating Higgs couplings [82]).

Of course, the Higgs boson is also produced via the same Higgs-strahlung and vector-boson fusion processes that operate at  $e^+e^-$  colliders. Thus, much of the LC program for Higgs physics is also possible at a  $\mu^+\mu^-$  collider. However, (presumably) reduced luminosities at the  $\mu^+\mu^-$  collider and backgrounds due to the decaying muons will degrade some of the LC precision Higgs measurements previously discussed.

### B. Probing EWSB at a Very Large Hadron Collider (VLHC)

If strong electroweak symmetry breaking, characterized by a scale of several TeV, is realized in nature, a proton collider with energies far above that of the LHC [96] will be a crucial instrument, complementary to multi-TeV lepton colliders, to study the dynamics of the system. The significance of quasi-elastic  $WW$  scattering signaling either the onset of the new strong interactions or the formation of new resonances, is greatly enhanced compared to the LHC, and it provides a motivation for detailed experimental studies.

If the Higgs boson is a composite particle, a proton collider with very high energies may be a unique instrument to search for its constituents. Examples include technicolor and top-color theories in which the new quarks may have masses of several TeV and above. For example, a condensate of  $\bar{Q}_{\text{TC}}Q_{\text{TC}}$  may be responsible for electroweak symmetry breaking, where  $Q_{\text{TC}}$  are techniquarks which make up the fundamental representation of an  $SU(4)$

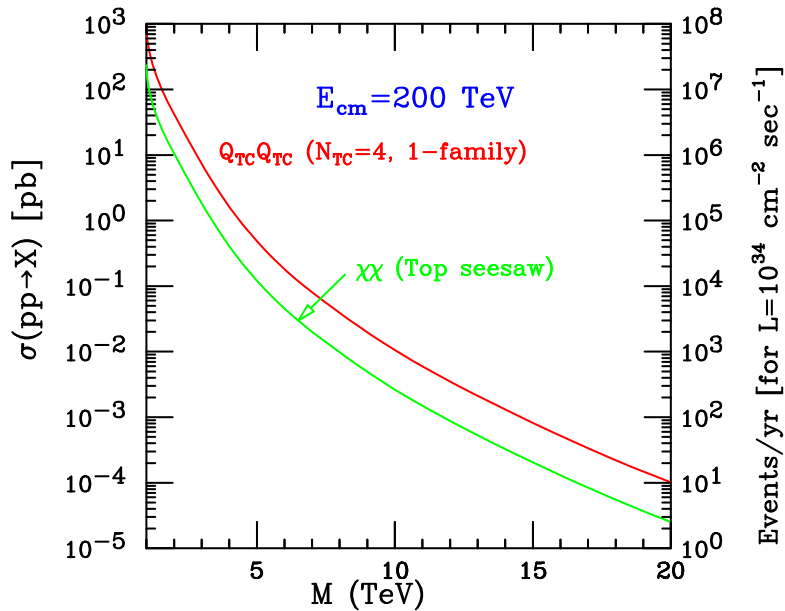


FIG. 10: The cross section for technicolor  $Q_{\text{TC}}$  pair production (solid line) and pair production of  $SU(2)_L$  singlet top-quark partners,  $\chi_L$  and  $\chi_R$ , in top-color models (dashed line) at the VLHC. The calculation assumes one degenerate isodoublet of techniquarks, and  $\chi_L$  and  $\chi_R$  are taken degenerate in mass. The right vertical scale shows the number of events per year, assuming a total yearly integrated luminosity of  $100 \text{ fb}^{-1}$ . Taken from Ref. [97].

technicolor group [10]. In the top-seesaw model of Ref. [13], the top quark and a novel weak  $SU(2)_L$  singlet quark  $\chi$  are responsible for the dynamical breaking of electroweak symmetry. The cross sections for production of these new particles at the VLHC are shown in Figure 10 [97]. However, detailed experimental studies of the signals and backgrounds in the hadronic environment are needed before firm conclusions can be drawn.

## V. CONCLUSIONS

The physical origin of electroweak symmetry breaking is not yet known. In all theoretical approaches and models, the dynamics of electroweak symmetry breaking must be revealed at the TeV-scale or below. This energy scale will be thoroughly explored by hadron colliders, starting with the Tevatron and followed later in this decade by the LHC. Even though the various theoretical alternatives can only be confirmed or ruled out by future collider experiments, a straightforward interpretation of the electroweak precision data suggests that electroweak symmetry breaking dynamics is weakly-coupled, and a Higgs boson with mass between 100 and 200 GeV must exist. With the supersymmetric extension of the Standard Model, this interpretation opens the route to grand unification of all the fundamental forces, with the eventual incorporation of gravity in particle physics. The observation of a light Higgs boson at the Tevatron or the LHC is the crucial first step. However, a high-luminosity  $e^+e^-$  collider, now under development, is needed to clarify the nature of the Higgs boson in a comprehensive form and to establish scalar sector dynamics as the mechanism *sui generis* for generating the masses of the fundamental particles. If strong electroweak symmetry breaking dynamics is realized in nature, supporting evidence can initially be extracted from experiments at the LHC and at an  $e^+e^-$  linear collider with  $\sqrt{s} = 500$  GeV—1 TeV, but the new strong interaction sector can only be fully explored at multi-TeV lepton and proton facilities.

In summary, discovering and interpreting new phenomena require energy frontier facilities and high precision capabilities. The search for the dynamics of electroweak symmetry breaking calls for colliders that probe energy scales from a few hundred GeV up to a TeV. Theoretical explanations of the mechanism of electroweak symmetry breaking demand new physics beyond the Standard Model at or near the TeV scale. There are fundamental questions concerning electroweak symmetry breaking and physics beyond the Standard Model that cannot be answered without a high energy physics program at an  $e^+e^-$  linear collider overlapping that of the LHC. Discoveries at these machines will elucidate the TeV scale, and they will pave the way for facilities that will explore new and higher energy frontiers at the multi-TeV scale.

## Acknowledgments

We would like to thank Jack Gunion, Sven Heinemeyer and Tom Rizzo for their careful reading of the manuscript and a number of useful suggestions. We also acknowledge fruitful conversations with JoAnne Hewett, Carlos Wagner, Georg Weiglein and Dieter Zeppenfeld. In addition, we greatly appreciate the contributions of the members of the Electroweak Symmetry Breaking (P1) working group participants, with special thanks to the P1 plenary speakers and subgroup conveners for their efforts. Finally, we are particularly grateful to Chris Quigg and the Snowmass Workshop organizing committee for inviting us to convene the P1 working group and for providing such a stimulating atmosphere.

Fermilab is operated by Universities Research Association, Inc. under contract no. DE-AC02-76CH03000 with the U.S. Department of Energy. D.W.G. is supported in part by an NSF Career award no. PHY-9818097 and

in part by the U.S. Department of Energy under grant no. DE-FG02-95ER20899. H.E.H. is supported in part by the U.S. Department of Energy under grant no. DE-FG03-92ER40689. A.S.T. acknowledges the support of U.S. Department of Energy contract no. DE-AC02-98CH10886.

---

[1] P.W. Higgs, Phys. Rev. Lett. **12**, 132 (1964); Phys. Rev. **145**, 1156 (1966); F. Englert and R. Brout, Phys. Rev. Lett. **13**, 321 (1964); G. S. Guralnik, C. R. Hagen, and T. W. B. Kibble, Phys. Rev. Lett. **13**, 585 (1964).

[2] S. Weinberg, Phys. Rev. **D13**, 974 (1979); **D19**, 1277 (1979); L. Susskind, Phys. Rev. **D20**, 2619 (1979).

[3] J.M. Cornwall, D.N. Levin and G. Tiktopoulos, Phys. Rev. Lett. **30**, 1268 (1973); Phys. Rev. **D10**, 1145 (1974); C.H. Llewellyn Smith, Phys. Lett. **46B**, 233 (1973).

[4] J.F. Gunion, H.E. Haber, G. Kane and S. Dawson, *The Higgs Hunter's Guide* (Perseus Publishing, Cambridge, MA, 2000).

[5] H.P. Nilles, Phys. Rep. **110**, 1 (1984); H.E. Haber and G.L. Kane, Phys. Rep. **117**, 75 (1985); S.P. Martin, hep-ph/9709356; P. Fayet, Nucl. Phys. Proc. Suppl. **101**, 81 (2001).

[6] G. 't Hooft, in *Recent Developments in Gauge Theories*, Proceedings of the NATO Advanced Summer Institute, Cargèse, 1979, edited by G. 't Hooft *et al.* (Plenum, New York, 1980) p. 135; M. Veltman, Acta Phys. Pol. **B12**, 437 (1981); E. Witten, Nucl. Phys. **B188**, 513 (1981); R.K. Kaul, Phys. Lett. **109B**, 19 (1982); Pramana **19**, 183 (1982); L. Susskind, Phys. Rep. **104**, 181 (1984).

[7] K. Inoue, A. Kakuto, H. Komatsu, and S. Takeshita, Prog. Theor. Phys. **68**, 927 (1982) [E: **70**, 330 (1983)]; **71**, 413 (1984); R. Flores and M. Sher, Ann. Phys. (NY) **148**, 95 (1983); J.F. Gunion and H.E. Haber, Nucl. Phys. **B272**, 1 (1986); **B278**, 449 (1986) [E: **B402**, 567 (1993)].

[8] M. Carena, J.R. Espinosa, M. Quiros and C.E.M. Wagner, Phys. Lett. **B355**, 209 (1995); M. Carena, M. Quiros and C.E.M. Wagner, Nucl. Phys. **B461**, 407 (1996); H.E. Haber, R. Hempfling and A.H. Hoang, Z. Phys. **C75**, 539 (1997); S. Heinemeyer, W. Hollik and G. Weiglein, Phys. Rev. **D58**, 091701 (1998); Phys. Lett. **B440**, 296 (1998); Eur. Phys. J. **C9**, 343 (1999); Phys. Lett. **B455**, 179 (1999); M. Carena, H.E. Haber, S. Heinemeyer, W. Hollik, C.E.M. Wagner and G. Weiglein, Nucl. Phys. **B580**, 29 (2000); J.R. Espinosa and R.-J. Zhang, JHEP **0003**, 026 (2000); Nucl. Phys. **B586**, 3 (2000); J.R. Espinosa and I. Navarro, Nucl. Phys. **B615**, 82 (2001); G. Degrassi, P. Slavich and F. Zwirner, Nucl. Phys. **B611**, 403 (2001); A. Brignole, G. Degrassi, P. Slavich and F. Zwirner, hep-ph/0112177.

[9] For a recent review, see C.T. Hill and E.H. Simmons, FERMI-PUB-02/045-T [hep-ph/0203079].

[10] E. Farhi and L. Susskind, Phys. Rep. **74** (1981) 277; R. K. Kaul, Rev. Mod. Phys. **55** (1983) 449; K. Lane, in *The Building Blocks of Creation—From Microfermis to Megaparsecs*, Proceedings of the Theoretical Advanced Study Institute (TASI 93) in Elementary Particle Physics, Boulder, CO, 6 June–2 July 1993, edited by S. Raby and T. Walker (World Scientific, Singapore, 1994).

[11] E.H. Simmons, “Technicolor evolution,” to appear in *Proc. of the APS/DPF/DPB Summer Study on the Future of Particle Physics* (Snowmass 2001), edited by R. Davidson and C. Quigg, hep-ph/0110196; K. Lane, two lectures presented at l'Ecole de GIF at LAPP, Annecy-le-Vieux, France, in September 2001, hep-ph/0202255.

[12] C.T. Hill, Phys. Lett. **B266**, 419 (1991); **B345**, 483 (1995);

[13] B.A. Dobrescu and C.T. Hill, Phys. Rev. Lett. **81**, 2634 (1998); R.S. Chivukula, B.A. Dobrescu, H. Georgi and C.T. Hill, Phys. Rev. **D59**, 075003 (1999); H.J. He, C.T. Hill and T.M. Tait, Phys. Rev. **D65**, 055006 (2002).

[14] I. Antoniadis, Phys. Lett. **B246**, 377 (1990); N. Arkani-Hamed, S. Dimopoulos and G.R. Dvali, Phys. Lett. **B429**, 263 (1998); L. Randall and R. Sundrum, Phys. Rev. Lett. **83**, 3370 (1999).

[15] For a recent review, see V.A. Rubakov, Phys. Usp. **44**, 871 (2001); Y.A. Kubyshin, Lectures given at 11th International School on Particles and Cosmology, Karbardino-Balkaria, Russia, 2001, hep-ph/0111027.

[16] G. Pásztor and T. Rizzo, “Report of the Snowmass Subgroup on Extra Dimensions,” to appear in *Proc. of the*

*APS/DPF/DPB Summer Study on the Future of Particle Physics* (Snowmass 2001), edited by R. Davidson and C. Quigg, hep-ph/0112054.

[17] B.A. Dobrescu, Phys. Lett. **B461**, 99 (1999); L.J. Hall and C. Kolda, Phys. Lett. **B459**, 213 (1999); H.C. Cheng, B.A. Dobrescu and C.T. Hill, Nucl. Phys. **B589**, 249 (2000).

[18] G.F. Giudice, R. Rattazzi and J.D. Wells, Nucl. Phys. **B595**, 250 (2001); M. Chaichian, A. Datta, K. Huitu and Z.Yu, Phys. Lett. **B524**, 161 (2002); J.L. Hewett and T.G. Rizzo, hep-ph/0202155. For a review of the properties of the radion, see G.D. Kribs, “Physics of the radion in the Randall-Sundrum scenario,” to appear in *Proc. of the APS/DPF/DPB Summer Study on the Future of Particle Physics* (Snowmass 2001), edited by R. Davidson and C. Quigg, hep-ph/0110242, and references therein.

[19] C. Csaki, M.L. Graesser and G. D. Kribs, Phys. Rev. **D63**, 065002 (2001); T. Han, G.D. Kribs and B. McElrath, Phys. Rev. **D64**, 076003 (2001); P. Das and U. Mahanta, Phys. Lett. **B528**, 253 (2002); C. Csaki, J. Erlich and J. Terning, hep-ph/0203034; J.L. Hewett, F.J. Petriello and T.G. Rizzo, hep-ph/0203091.

[20] D. Abbaneo *et al.* [LEP Electroweak Working Group] and N. de Groot *et al.* [SLD Heavy Flavor and Electroweak Groups], CERN-EP/2001-098 [hep-ex/0112021] and additional updates at <http://lepewg.web.cern.ch/LEPEWWG>.

[21] U. Baur, R. Clare, J. Erler, S. Heinemeyer, D. Wackerth, G. Weiglein and D.R. Wood, “Theoretical and experimental status of the indirect Higgs boson mass determination in the Standard Model,” to appear in *Proc. of the APS/DPF/DPB Summer Study on the Future of Particle Physics* (Snowmass 2001), edited by R. Davidson and C. Quigg, hep-ph/0111314.

[22] R. Barbieri and A. Strumia, Phys. Lett. **B462**, 144 (1999); R. S. Chivukula and N. Evans, Phys. Lett. B **464**, 244 (1999); J.A. Bagger, A.F. Falk and M. Swartz, Phys. Rev. Lett. **84**, 1385 (2000); C. Kolda and H. Murayama, JHEP **0007**, 035 (2000).

[23] R. Casalbuoni, S. De Curtis, D. Dominici, R. Gatto and M. Grazzini, Phys. Lett. B **435**, 396 (1998); L.J. Hall and C. Kolda, Phys. Lett. **B459**, 213 (1999); T.G. Rizzo and J.D. Wells, Phys. Rev. **D61**, 016007 (2000); R.S. Chivukula, C. Hoelbling and N. Evans, Phys. Rev. Lett. **85**, 511 (2000); P. Chankowski, T. Farris, B. Grzadkowski, J.F. Gunion, J. Kalinowski and M. Krawczyk, Phys. Lett. **B496**, 195 (2000); H.J. He, N. Polonsky and S.F. Su, Phys. Rev. **D64**, 053004 (2001); M.E. Peskin and J.D. Wells, Phys. Rev. **D64**, 093003 (2001).

[24] G. Altarelli, F. Caravaglios, G.F. Giudice, P. Gambino and G. Ridolfi, JHEP **0106**, 018 (2001); M.S. Chanowitz, Phys. Rev. Lett. **87**, 231802 (2001); D. Choudhury, T.M. Tait and C.E.M. Wagner, Phys. Rev. **D65**, 053002 (2002); S. Davidson, S. Forte, P. Gambino, N. Rius and A. Strumia, JHEP **0202**, 037 (2002).

[25] L.E. Ibáñez and G.G. Ross, Phys. Lett. **B105**, 439 (1981); S. Dimopoulos, S. Raby, F. Wilczek, Phys. Rev. **D24**, 1681 (1981); M.B. Einhorn and D.R.T. Jones, Nucl. Phys. **B196**, 475 (1982); W.J. Marciano and G. Senjanovic, Phys. Rev. **D25**, 3092 (1982).

[26] J. Ellis, S. Kelley and D.V. Nanopoulos, Phys. Lett. **B249**, 441 (1990); P. Langacker and M. Luo, Phys. Rev. **D44**, 817 (1991); U. Amaldi, W. de Boer and H. Fürstenau, Phys. Lett. **B260**, 447 (1991); P. Langacker and N. Polonsky, Phys. Rev. **D52**, 3081 (1995); S. Pokorski, Acta Phys. Polon. **B30**, 1759 (1999). For a recent review, see: R.N. Mohapatra, in *Particle Physics 1999*, ICTP Summer School in Particle Physics, Trieste, Italy, 21 June–9 July, 1999, edited by G. Senjanovic and A.Yu. Smirnov. (World Scientific, Singapore, 2000) pp. 336–394.

[27] ALEPH, DELPHI, L3 and OPAL Collaborations [LEP Higgs Working Group for Higgs boson searches Collaboration], hep-ex/0107029, and additional updates at <http://lephiggs.web.cern.ch/LEPHIGGS/www/Welcome.html>.

[28] M. Carena, J.S. Conway, H.E. Haber, J. Hobbs *et al.*, Report of the Tevatron Higgs Working Group, hep-ph/0010338.

[29] P.C. Bhat, R. Gilmartin and H.B. Prosper, Phys. Rev. **D62**, 074022 (2000).

[30] T. Han, A.S. Turcot and R.-J. Zhang, Phys. Rev. **D59**, 093001 (1999).

[31] ATLAS Collaboration, Technical Design Report, CERN-LHCC 99-14; CMS Collaboration, Technical Proposal, CERN-LHCC 94-38.

[32] J.G. Branson, D. Denegri, I. Hinchliffe, F. Gianotti, F.E. Paige and P. Sphicas, BNL-HET-01/33 [hep-ph/0110021].

[33] D. Cavalli *et al.*, Report of the Higgs working group for the Workshop “Physics at TeV Colliders,” Les Houches,

France, 21 May–1 June 2001, hep-ph/0203056.

[34] J. Conway, K. Desch, J.F. Gunion, S. Mrenna and D. Zeppenfeld, Report of the P1-WG2 subgroup, “The Precision of Higgs Boson Measurements and their Implications,” to appear in *Proc. of the APS/DPF/DPB Summer Study on the Future of Particle Physics* (Snowmass 2001), edited by R. Davidson and C. Quigg, hep-ph/0203206.

[35] T. Trefzger, “Search for Higgs Bosons at LHC,” to appear in *Proc. of the APS/DPF/DPB Summer Study on the Future of Particle Physics* (Snowmass 2001), edited by R. Davidson and C. Quigg.

[36] M. Spira, *Fortsch. Phys.* **46**, 203 (1998); S. Dawson, “Higgs boson production rates in hadronic collisions,” to appear in *Proc. of the APS/DPF/DPB Summer Study on the Future of Particle Physics* (Snowmass 2001), edited by R. Davidson and C. Quigg, hep-ph/0111226.

[37] W. Beenakker, S. Dittmaier, M. Kramer, B. Plumper, M. Spira and P. M. Zerwas, *Phys. Rev. Lett.* **87**, 201805 (2001); L. Reina and S. Dawson, *Phys. Rev. Lett.* **87**, 201804 (2001).

[38] M. Dittmar and H. Dreiner, *Phys. Rev.* **D55**, 167 (1997); D. Rainwater and D. Zeppenfeld, *Phys. Rev.* **D60**, 113004 (1999) [E: **D61**, 099901 (1999)]; N. Kauer, T. Plehn, D. Rainwater and D. Zeppenfeld, *Phys. Lett.* **B503**, 113 (2001).

[39] D. Zeppenfeld, R. Kinnunen, A. Nikitenko and E. Richter-Was, *Phys. Rev.* **D62**, 013009 (2000); D. Zeppenfeld, “Higgs Couplings at the LHC,” to appear in *Proc. of the APS/DPF/DPB Summer Study on the Future of Particle Physics* (Snowmass 2001), edited by R. Davidson and C. Quigg, hep-ph/0203123.

[40] T. Plehn, D. Rainwater and D. Zeppenfeld, *Phys. Rev. Lett.* **88**, 051801 (2002).

[41] E. Richter-Was and M. Sapinski, *Acta Phys. Polon.* **B30**, 1001 (1999); M. Sapinski and D. Cavalli, *Acta Phys. Polon.* **B32**, 1317 (2001).

[42] D. Green, K. Maeshima, R. Vidal and W. Wu, CMS NOTE 2001/039; D. Green, K. Maeshima, R. Vidal, W. Wu and S. Kunori, FERMILAB-FN-0705 (2001); V. Drollinger, Th. Müller and D. Denegri, CMS NOTE 2001/054 [hep-ph/0111312].

[43] U. Baur *et al.*, Report of the P1-WG1 subgroup, “Present and Future Electroweak Precision Measurements and the Indirect Determination of the Mass of the Higgs Boson,” to appear in *Proc. of the APS/DPF/DPB Summer Study on the Future of Particle Physics* (Snowmass 2001), edited by R. Davidson and C. Quigg, hep-ph/0202001.

[44] H.E. Haber and R. Hempfling, *Phys. Rev. Lett.* **66**, 1815 (1991); Y. Okada, M. Yamaguchi and T. Yanagida, *Prog. Theor. Phys.* **85**, 1 (1991); J. Ellis, G. Ridolfi and F. Zwirner, *Phys. Lett.* **B257**, 83 (1991).

[45] M. Carena, S. Mrenna and C. E. Wagner, *Phys. Rev.* **D62**, 055008 (2000).

[46] S. Dimopoulos and H. Georgi, *Nucl. Phys.* **B193**, 150 (1981); K. Harada and N. Sakai, *Prog. Theor. Phys.* **67**, 1877 (1982); K. Inoue, A. Kakuto, H. Komatsu and S. Takeshita, *Prog. Theor. Phys.* **67**, 1889 (1982); L. Girardello and M.T. Grisaru, *Nucl. Phys.* **B194**, 65 (1982); L.J. Hall and L. Randall, *Phys. Rev. Lett.* **65**, 2939 (1990); I. Jack and D.R.T. Jones, *Phys. Lett.* **B457**, 101 (1999).

[47] B.C. Allanach *et al.*, “The Snowmass points and slopes: Benchmarks for SUSY searches,” to appear in *Proc. of the APS/DPF/DPB Summer Study on the Future of Particle Physics* (Snowmass 2001) edited by R. Davidson and C. Quigg, hep-ph/0202233.

[48] T. L. Barklow, R. S. Chivukula, J. Goldstein and T. Han, Report of the P1-WG4 subgroup, “Electroweak symmetry breaking by strong dynamics and the collider phenomenology,” to appear in *Proc. of the APS/DPF/DPB Summer Study on the Future of Particle Physics* (Snowmass 2001), edited by R. Davidson and C. Quigg, hep-ph/0201243.

[49] R. Casalbuoni, A. Deandrea, S. De Curtis, D. Dominici, R. Gatto and J. F. Gunion, *Nucl. Phys.* **B555**, 3 (1999).

[50] N. Akasaka *et al.*, “JLC design study,” KEK-REPORT-97-1. The present status of the JLC machine parameters were presented by K. Yokoya, <http://lcdev.kek.jp/Reviews/LCPAC2002/LCPAC2002.KY.pdf> (March, 2002).

[51] C. Adolphsen *et al.* [International Study Group Collaboration], “International study group progress report on linear collider development,” SLAC-R-559 and KEK-REPORT-2000-7 (April, 2000).

[52] R. Brinkmann, K. Flottmann, J. Rossbach, P. Schmuser, N. Walker and H. Weise [editors], “TESLA: The superconducting electron positron linear collider with an integrated X-ray laser laboratory. Technical design report, Part 2: The Accelerator,” DESY-01-011 (March, 2001), <http://tesla.desy.de/tdr/>.

[53] R.W. Assmann *et al.* [The CLIC Study Team], “A 3 TeV  $e^+e^-$  linear collider based on CLIC technology,” edited by G. Guignard, SLAC-REPRINT-2000-096 and CERN-2000-008. A parameter summary and general layout of the CLIC complex for  $\sqrt{s} = 5$  TeV is also provided in an appendix to this report.

[54] R.D. Heuer, D.J. Miller, F. Richard and P.M. Zerwas [editors], “TESLA: The superconducting electron positron linear collider with an integrated X-ray laser laboratory. Technical design report, Part 3: Physics at an  $e^+e^-$  Linear Collider,” DESY-01-011 (March, 2001), <http://tesla.desy.de/tdr/> [hep-ph/0106315].

[55] American Linear Collider Working Group, T. Abe *et al.*, SLAC-R-570 (2001), hep-ex/0106055-58.

[56] ACFA Linear Collider Working Group, K. Abe *et al.*, KEK-REPORT-2001-11 (2001), hep-ph/0109166.

[57] J. Brau, C. Potter and M. Iwasaki, Workshop on Physics and Detectors for Future  $e^+e^-$  Linear Colliders, Johns Hopkins University, 2001.

[58] D.J. Miller, S.Y. Choi, B. Eberle, M.M. Mühlleitner and P.M. Zerwas, Phys. Lett. **B505**, 149 (2001); P. Garcia, W. Lohmann and A. Raspereza, LC-Note LC-PHSM-2001-054.

[59] M. Battaglia and K. Desch, in *Physics and experiments with future linear  $e^+e^-$  colliders*, Proceedings of the 5th International Linear Collider Workshop, Batavia, IL, USA, 2000, edited by A. Para and H.E. Fisk (American Institute of Physics, New York, 2001), pp. 163–182 [hep-ph/0101165].

[60] S. Dittmaier, M. Kramer, Y. Liao, M. Spira and P.M. Zerwas, Phys. Lett. **B441**, 383 (1998).

[61] A. Juste and G. Merino, hep-ph/9910301; H. Baer, S. Dawson and L. Reina, Phys. Rev. **D61**, 013002 (2000).

[62] A. Djouadi, W. Kilian, M.M. Mühlleitner and P.M. Zerwas, Eur. Phys. J. **C10**, 27 (1999); C. Castanier, P. Gay, P. Lutz and J. Orloff, LC Note LC-PHSM-2000-061 [hep-ex/0101028].

[63] A. Djouadi, H.E. Haber and P.M. Zerwas, Phys. Lett. **B375**, 203 (1996); J. Kamoshita, Y. Okada, M. Tanaka and I. Watanabe, hep-ph/9602224; D.J. Miller and S. Moretti, Eur. Phys. J. **C13**, 459 (2000).

[64] D. Choudhury, T.M. Tait and C.E.M. Wagner, ANL-HEP-PR-02-018 [hep-ph/0202162].

[65] J. Alcaraz and E. Ruiz Morales, Phys. Rev. Lett. **86**, 3726 (2001).

[66] I.F. Ginzburg, G.L. Kotkin, S.L. Panfil, V.G. Serbo, V.I. Telnov, Nucl. Instrum. Meth. **A219**, 5 (1984);

[67] E. Boos *et al.*, Nucl. Instrum. Meth. **A472**, 100 (2001).

[68] D.L. Borden, D.A. Bauer and D.O. Caldwell, Phys. Rev. **D48**, 4018 (1993); J.F. Gunion and H.E. Haber, Phys. Rev. **D48**, 5109 (1993).

[69] S. Söldner-Rembold and G. Jikia, Nucl. Instrum. Meth. A **472**, 133 (2001); M. Melles, Nucl. Instrum. Meth. A **472**, 128 (2001).

[70] D.M. Asner, J.B. Gronberg and J.F. Gunion, hep-ph/0110320.

[71] M.M. Velasco *et al.*, “Photon-Photon and Electron-Photon Colliders with Energies Below a TeV,” to appear in *Proc. of the APS/DPF/DPB Summer Study on the Future of Particle Physics* (Snowmass 2001), edited by R. Davidson and C. Quigg, hep-ph/0111055.

[72] J. Erler, S. Heinemeyer, W. Hollik, G. Weiglein and P.M. Zerwas, Phys. Lett. **B486**, 125 (2000); J. Erler and S. Heinemeyer, in *Proceedings of the 5th International Symposium on Radiative Corrections* (RADCOR 2000), edited by H.E. Haber, hep-ph/0102083.

[73] P. Langacker and H.A. Weldon, Phys. Rev. Lett. **52**, 1377 (1984); H.A. Weldon, Phys. Rev. **D30**, 1547 (1984); J.F. Gunion, H.E. Haber and J. Wudka, Phys. Rev. **D43**, 904 (1991); J.F. Gunion, B. Grzadkowski, H.E. Haber and J. Kalinowski, Phys. Rev. Lett. **79**, 982 (1997).

[74] H.E. Haber and Y. Nir, Nucl. Phys. **B335**, 363 (1990); H.E. Haber, in *Physics From the Planck Scale to the Electroweak Scale*, Proceedings of the US–Polish Workshop, Warsaw, Poland, 1994, edited by P. Nath, T. Taylor, and S. Pokorski (World Scientific, Singapore, 1995), pp. 49–63; J.F. Gunion and H.E. Haber, in preparation.

[75] M. Carena, H.E. Haber, H.E. Logan and S. Mrenna, Phys. Rev. **D65**, 055005 (2002).

[76] M.M. Mühlleitner, M. Krämer, M. Spira and P.M. Zerwas, Phys. Lett. **B508**, 311 (2001).

[77] See, *e.g.*, U. Ellwanger, M. Rausch de Traubenberg, and C.A. Savoy, Nucl. Phys. **B492**, 21 (1997), and references therein.

- [78] J. Kamoshita, Y. Okada and M. Tanaka, Phys. Lett. **B328**, 67 (1994).
- [79] J.R. Espinosa and J.F. Gunion, Phys. Rev. Lett. **82**, 1084 (1999).
- [80] U. Ellwanger, J.F. Gunion and C. Hugonie, hep-ph/0111179; J.F. Gunion, H.E. Haber and T. Moroi, in *New Directions for High Energy Physics*, Proceedings of the 1996 DPF/DPB Summer Study on High Energy Physics, Snowmass '96, edited by D.G. Cassel, L.T. Gennari and R.H. Siemann (Stanford Linear Accelerator Center, Stanford, CA, 1997) pp. 598–602.
- [81] J. Gunion, T. Han, J. Jiang, S. Mrenna and A. Sopczak, “Determination of  $\tan \beta$  at a Future  $e^+e^-$  Linear Collider,” to appear in *Proc. of the APS/DPF/DPB Summer Study on the Future of Particle Physics* (Snowmass 2001), edited by R. Davidson and C. Quigg, hep-ph/0112334.
- [82] A. Pilaftsis, Phys. Rev. **D58**, 096010 (1998); Phys. Lett. **B435**, 88 (1998); A. Pilaftsis and C.E.M. Wagner, Nucl. Phys. **B553**, 3 (1999); D.A. Demir, Phys. Rev. **D60**, 055006 (1999); S.Y. Choi, M. Drees and J.S. Lee, Phys. Lett. **B481**, 57 (2000); M. Carena, J.R. Ellis, A. Pilaftsis and C.E.M. Wagner, Phys. Lett. **B495**, 155 (2000); Nucl. Phys. **B586**, 92 (2000); **B625**, 345 (2002); S. Heinemeyer, Eur. Phys. J. **C22**, 521 (2001).
- [83] J.F. Gunion, H.E. Haber and J. Kalinowski, in preparation.
- [84] T.L. Barklow, “Strong symmetry breaking at  $e^+e^-$  linear colliders,” to appear in *Proc. of the APS/DPF/DPB Summer Study on the Future of Particle Physics* (Snowmass 2001), edited by R. Davidson and C. Quigg, hep-ph/0112286.
- [85] E. Boos, H.-J. He, A. Pukhov, W. Kilian, C.P. Yuan and P.M. Zerwas, Phys. Rev. **D57**, 1553 (1998); **D61**, 077901 (2000).
- [86] K. Lane, K.R. Lynch, S. Mrenna, E.H. Simmons, hep-ph/0203065.
- [87] V.D. Barger, M.S. Berger, J.F. Gunion and T. Han, Phys. Rep. **286**, 1 (1997).
- [88] C. Ankenbrandt *et al.*, Phys. Rev. ST Accel. Beams **2**, 081001 (1999).
- [89] Prospective Study of Muon Storage Rings at CERN, B. Autin, A. Blondel and J.R. Ellis (*eds.*), CERN-99-02 (1999).
- [90] V.D. Barger, M. Berger, J.F. Gunion and T. Han, “Physics of Higgs factories,” to appear in *Proc. of the APS/DPF/DPB Summer Study on the Future of Particle Physics* (Snowmass 2001), edited by R. Davidson and C. Quigg, hep-ph/0110340.
- [91] M.S. Berger, “Higgs Bosons at Muon Colliders,” to appear in *Proc. of the APS/DPF/DPB Summer Study on the Future of Particle Physics* (Snowmass 2001), edited by R. Davidson and C. Quigg, hep-ph/0110390.
- [92] C. Blöchinger *et al.*, *Physics Opportunities at  $\mu^+\mu^-$  Higgs Factories*, CERN-TH/2002-028 [hep-ph/0202199].
- [93] D. Atwood and A. Soni, Phys. Rev. **D52**, 6271 (1995).
- [94] M. Kramer, J.H. Kuhn, M.L. Stong and P.M. Zerwas, Z. Phys. **C64**, 21 (1994); B. Grzadkowski and J.F. Gunion, Phys. Lett. **B350**, 218 (1995).
- [95] B. Grzadkowski, J.F. Gunion and J. Pliszka, Nucl. Phys. **B583**, 49 (2000).
- [96] P. Limon *et al.* [VLHC Design Study Group], “Design Study for a Staged VLHC,” Fermilab-TM-2149 (May, 2001); M. Blaskiewicz *et al.*, “VLHC Accelerator Physics,” FERMILAB-TM-2158 (November, 2001).
- [97] U. Baur, R. Brock and J. Parsons *et al.*, Report of the E4 Working Group, “Physics at Future Hadron Colliders,” to appear in *Proc. of the APS/DPF/DPB Summer Study on the Future of Particle Physics* (Snowmass 2001), edited by R. Davidson and C. Quigg, hep-ph/0201227.